Part VI

Symbiotics and Other Related Systems

ROSAT Observations of Symbiotic Binaries and Related Objects

K.F. Bickert[1], J. Greiner[1], R.E. Stencel[2]

[1] Max-Planck-Institut für extraterrestrische Physik, Garching FRG
[2] Department of Physics and Astronomy, University of Denver, Denver CO

Abstract. We present X-ray observations of 217 confirmed or suspected symbiotic binaries with the ROSAT PSPC during the all-sky survey and 129 archived pointings. A table lists 3σ upper limits or detected count rates for survey and pointing observations (available for 46 objects) plus a collection of UBVJHK brightnesses, stellar types, outburst status, and structure (jets, ejecta, winds, clouds). The detection of 28 symbiotics (21 in survey) will be handled in greater detail in a forthcoming paper.

1 Introduction

Symbiotic stars form a heterogeneous class of long period, interacting binaries hosting a cool red giant (K- or M-class or Mira) and a hot compact subdwarf, white dwarf, or neutron star (Mikolajewska and Kenyon 1992). They are strong UV emitters, but *Einstein* and *EXOSAT* observatories detected only a few systems (Allen 1981) of a small subset (ca. 25) observed, presumably due to circumbinary and interstellar reddening. The ROSAT all-sky survey provides the first statistically complete sampling of the more than 200 objects. Long exposure pointings added to detections, improved statistsics and show sometimes drastic time variation of the X-ray emission.

A key question in symbiotics is the source of the high energy radiation, whether it is a) thermal radiation from the compact companion surface, or b) compact's photosphere, or c) from a possible accretion disk or d) its corona, e) from a heated outburst shell, or f) collisional excitation from e.g. stellar wind shock regions, or g) from the giant's corona. X-ray observations reveal the most energetic regions in the system (10–30 eV typ.), spectra and variability should help assigning models to individual systems.

2 Observations

The German X-ray satellite ROSAT (cf. Trümper 1984) hosts two imaging telescopes: the UK EUV wide field camera, and the German soft X-ray telescope (XRT). The XRT mirrors feed MPE's Position Sensitive Proportional Counters (PSPC-C and -B, 4 color energy resolution) and the US SAO's High Resolution Imager (HRI, b/w). Here we used only PSPC data because of higher sensitivity and better background rejection at low energies. EUV detected EX Hya (in a pointing) and (marginally) AG Dra (in the all-sky survey).

We have examined the survey data for detections from a list of 212 symbiotic and symbiotic-like objects compiled by Allen (1984), Kenyon (1986), Vaidis (1988) and others. For completeness we included all sources that may be or might have been symbiotics. Some of the objects might need reobservations to confirm their status, some might be mis-classified planetary nebulae, contain super-giants or their assignment may simply be in error. Some may have changed type due to outbursts or evolution. We include a flag denoting the confirmation status.

The ROSAT all-sky survey covered 96% of the sky. For 208 objects all-sky survey data were available (exposure > 32 sec). We used EXSAS V4.0 standard survey procedures on 40 x 40 arcmin fields around the candidate source positions (involving a local detect algorithm for channels 11–235, using a 5 arcmin cutradius; sources with a likelihood > 8 were cut out the data before calculating the local background map; reading supplied exposure map for dead-time and vignetting corrected time). Two maximum likelihood upper limit runs with fixed and free position fits at 3σ confidence level and a detection threshold of ML > 6 delivered upper limit or source counts plus error. For detected sources, the distance between the optical and free fit X-ray position was calculated. The analysis of bright X-ray sources suggests that PSPC positions can be accurately determined to within 30 arcsec, and to less than 1 arcmin for soft and weak sources. Source confusion may disturb our results for LMC S63 (HV 12671).

We performed a number of follow-up pointed observations on symbiotic stars which were detected in the all-sky survey above at least 2σ. There were also pointings by other observers on stars from our list, either on purpose or coincidentally within a search radius of 30 arcmin. Beyond 35 arcmin, weak soft sources are difficult to detect due to blurring and the upper limit determination gets unreliable due to possible source confusion and problems in the background determination. A total of 129 such datasets are available (now in the ROSAT archive) covering 46 stars. Due to off-center pointings, 4 objects fall outside of our 30 arcmin detection area and thus have no pointing entries in the table.

3 Results List

The results were compacted to a table with 21 columns (described next) and 217 double line rows, sorted by right ascension.

1: sequential number

2: One or two most popular names (some objects have up to 14), variable star notation was preferred.

3: Flags:

c - symbiotic confirmation status (t -true, s - suspected, blank - unknown)

i - mid-infrared excess $= 25\mu/12\mu$ IRAS class (D dusty or S stellar)

j - jet flag set if any extended structure known (j jet, o optical, i infrared, r radio)

bur - burst type (rn - recurrent nova, sn - slow nova, bu - some outburst detected)

4-6: Coordinates:
right ascension + declination epoch 2000.0 fk5,
galactic (system II) longitude l and latitude b
ecliptic latitude (estimates survey visibility)
survey total coverage [sec] = upper limit for survey exposure
7-13: Count rates (upper line pointing results, lower line survey):
detection flag: u upper limit, d 3σ detection (ml >= 6.)
maximum likelihood for point source existence (from source detection)
(ml >= $14.3 = 5\sigma, 9.65 = 4\sigma, 5.91 = 3\sigma, 3.08 = 2\sigma$)
source count rate in [1/sec] if detected, else upper limit rate
(vignetting and dead-time corrected)
rate error scaled to [1/1000sec]. only for detections
actual exposure time (vignetting and dead-time corrected)
positon offset determined with parameter free (in compute/upper) [arcsec]
observation dates [yymmddxmmdd]
(x = - if dates span < 1 year, + if <2, or a digit)
14 top: offcenter, distance between pointing position and symbiotic in [arcmin]
14 bot: structure flags: denote if star has any known extended structures
(j-jet, e-ejecta, w-wind, c-clouds, x-complex, b-eclipse)
15 top: hydrogen column density nH in [10^{20} / cm^2]
15 bot: jet, optical, infrared, or radio diameter in [arcsec]
16: stellar types of red and blue component
17-19: brightness in UBV and JHK bands in [magnitudes] (c is color mag)
20 top: year or Julian date of outburst (slow or recurrent nova or other)
20 bot: estimates of stellar distance [kpc]
21: References: 1-Allen 1980, 2-Paresce 1990, 3-Kenny et al. 1991, 4-Burgarella & Paresce 1991, 5-Leedyarv 1989, 6-Whitelock 1988, 7-Taylor 1988, 8-Schulte-Ladbeck 1988, 9-Kenyon 1988, 10-Anandaro et al. 1988, 11-Solf 1984, 12-Kohoutek 1987, 13-Viotti 1988, 14-Downes & Shara 1993, 15-Kholopov et al. 1985, 16-Kenyon & Truran 1983, 17-Kenyon 1986, 18-Vaidis 1988, 19-Luthardt 1992, 20-Argelander, 21-Perek & Kohoutek 1967, 22-Kholopov et al. 1987, 23-Acker et al. 1982, 24-Kholopov 1982, 25-Henize 1976, 26-Cannon & Pickering, 27-Sanduleak & Stephenson 1973, 28-SIMBAD catalogue, 29-Whitelock 1988, 30-Gezari et al. 1993, 31-Inca consortium 1992.

All structural, burst, and brightness information was taken from the literature. The data are not completely up to date (literature search stopped mid 1994), especially as the stars are often highly variable and may undergo substantial changes in stellar type and brightness within few months or years. Reported are changes of appearance from symbiotic to planetary nebulae and back within a few months. If dates of acquired information was given, the year was appended (value'year). If data was unsecure, a question mark was added. The data is highly incomplete, mostly due to a real lack of observations of the stars, but also in part due to lack of time devoted to searching data. Search has been resumed for the detected stars.

4 Analysis

We tried correlations of the X-ray count rate of all sources with an ML above 6 (3σ, 28 objects), 3 (2σ, 49) or 2 (1.5σ, 71) with any of the data collected from the literature. We only summarize here the first results, a deeper study of the detections is in preparation, where we also discuss previous observations. A preliminary version is available.

Too few data were cited on the stellar type of the compact object, on U magnitude or UV brightness. On B mags, information was too often imprecise of whether absorption and reddening was included or not, completely upsetting results. No significant correlation to the stellar class of the giant and the V, J, H, K magnitudes was found. For IRAS infrared classification, 6/8/8 of 24 dusty systems were detected versus 10/22/37 of 107 stellars. When corrected for distance and N_H, there also seems to be no correlation.

Information on the spatial structure (jets, ejecta, winds, clouds) is scarce (stars must be well within 1 kpc distance), but 8/9/9 out of 11 objects were detected. 7/8/10 of 17 bursters are seen, those nearby or with low N_H and in later outburst phases (AG Dra is absorbed in beginning, no others seen in early phase). A few sources found by Einstein/EXOSAT were now below detection level, even in deep pointing.

Symbiotics seem not to be standard candles, neither within nova (4 comparable) or steady burner group (5). A rough logN/logS shows strong deviation from powerlaw (but bad statistic).

Their high known variability in the radio, infrared, optical, and UV is also seen in soft X-rays: up to a factor of 300 (EX Hya), mean factor of 4 of 23 compared (without EX Hya) on time scale of 1..3 years (survey to pointing). Only 7 keep their level.

Most stars detected are within 1–2 kpc stellar distance, and the 3 which are further away have a hard spectrum. Typical spectra are very soft (10–25 eV) (the only really hard one, GX 1+4, harbours a neutron star). Neither blackbody nor powerlaw models fit the X-ray spectra well. Better fits are sometimes achieved by detailed white dwarf atmosphere model with or without winds (e.g. Mürset et al. 1996).

No straightforward support of any of the possible emission mechanisms is possible. Too few detections are comparable without in-depth model studies. Symbiotics are too heterogeneous.

Symbiotics cluster in the Galactic plane/center and are strongly affected by galactic and (in some systems high) intrinsic reddening and absorption. Accounting for distance and absorbing column, one would expect to detect X-ray emission only from a minor fraction of our sample of symbiotics. The fairly high detection rate among this subsample in the all-sky survey and pointed observations suggests, that all symbiotic systems emit X-ray emission at some level.

Acknowledgement: JG is supported by the Deutsche Agentur für Raumfahrtangelegenheiten (DARA) GmbH under contract FKZ 50 OR 9201. The ROSAT

project is supported by the German Bundesministerium für Bildung, Forschung, Wissenschaft und Technik (BMBW/DARA) and the Max-Planck-Society. We made use of the SIMBAD database, operated at CDS, Strasbourg France.

References

Acker A., et al. ., 1982, Publ. Spec. CDS. No. 3
Allen D.A., 1980, MNRAS 192, 521
Allen D., 1981, MNRAS 197, 739 (erratum MNRAS 201, 1199)
Allen D., 1984, Proc. Astron. Soc. Austral. 5, 369
Anandaro B.G., Taylor A.R., Pottasch S.R., 1988, A&A 203, 361
Anderson C., Cassinelli J., Sanders W., 1981, ApJ 247, L127
Argelander F.W.A., Bonner Durchmusterung
Burgarella D., Paresce F., 1991, ApJ 370, 590
Cannon A.J., Pickering E.C., Henry Draper Memorial HD catal.
Cassatella A., et al. 1984, ApSS 131, 763
Cordova F., Mason K., 1984, MNRAS 206, 879
Downes R.A., Shara M.M., 1993, PASP 105, 127
Gezari D.Y., et.al. 1993, NASA Ref. Pub. 1294, Cat. of Infrared Observations
Henize K.G., 1976, ApJ Suppl. 30, 491
inca consortium: 1992, ESA SP-1136, Hipparcos input catalogue
Jura M., Helfand D., 1984, ApJ 287, 785
Kenny H.T., Taylor A.R. Seaquist E.R., 1991, ApJ 366, 549
Kenyon S.J., 1986, The Symbiotic Stars (Cambridge)
Kenyon S.J., 1988, AJ 96, 337
Kenyon S.J., Truran J.W., 1983, ApJ 273, 280
Kenyon S., Fernandez-Castro T., Stencel R., 1988, AJ 95, 1817
Kholopov P.N. (ed.), 1982 NSV New catal o Suspected Variable Stars
Kholopov P.N. (ed.), 1985, General Catalogue of Variable Stars (GCVS)
Kholopov P.N. (ed.), 1987, General Catalogue of Variable Stars II
Kohoutek L., 1987, ApSS 131, 781
Leahy D., Taylor A., 1987, A&A 176, 302
Leedyarv L.E., 1989, Ap 31, 598
Luthardt R., 1992, Measurements from the Sonneberg Plate Archive (priv. comm.)
Mikolajewska J., Kenyon S., 1992, MNRAS 256, 177
Mürset U., Jordan S., Wolff B., 1996, this volume p. 251
Nussbaumer H., Vogel M., 1990, A&A 236, 117
Paresce F., 1990, ApJ 357, 231
Perek L., Kohoutek L., 1967, Catal. Galactic Planetary Nebulae, Czechosl.
Sanduleak N., Stephenson C.B., 1973, ApJ 185, 899
Schulte-Ladbeck R., 1988, AAp 189, 97
Solf J., 1984, A&A 139, 296
Taylor A.R., 1988, in The Symbiotic Phenomenon, ed. J. Mikolajewska, p. 77
Trümper J., 1984, Phys. Scripta T7, 209
Vaidis J.P., 1988, Bull. Astron. Franc. Obs. Etoiles Var. No.45/3+ff
Viotti R., 1988, in The Symbiotic Phenomenon, ed. J. Mikolajewska, p. 269
Viotti R., Piro L., Friedjung M., Cassatella A., 1987, ApJ 319, L7
Whitelock P., 1988, in The Symbiotic Phenomenon, ed. J. Mikolajewska, p. 47

Table 1. ROSAT Observations of Symbiotic Stars

seq	name.....	cij	ra.[e2000]	.....dec	....ecl	P	mlik	.prate	perr	pexpo	pxoff
	name-2.....	bur	..gal.lII.	.gal.bII.	surexpo	S	mlik	.srate	serr	sexpo	sxoff
1	V641 Cas	t	00h09m26s4	$+63d57m14$	54.797						
			118.341	1.457	582.0	u	0.9	0.0066		430.4	
2	V410 Cas	t	00h23m27s8	$+61d46m28$	52.108						
			119.630	−0.918	673.9	u	0.0	0.0158		492.6	
3	SMC1	t	00h29m10s8	$-74d57s40$	−64.048						
			304.877	−42.083							
4	SMC2	t	00h42m48s2	$-74d42m01$	−64.750						
			303.704	−42.415							
5	EG And	tS	00h44m37s2	$+40d40m46$	32.662	u	3.6	0.0063		8037.7	
	HD 4174		121.537	−22.174	510.0	u	3.1	0.0089		492.5	
6	SMC3	t	00h48m20s8	$-73d31m53$	−64.615						
			303.237	−43.595							
7	SMC-S 18		00h54m09s4	$-72d41m51$	−64.643	u	0.4	0.0009		69799	
	LHA 115-S 18		302.650	−44.429	483.3	u	0.9	0.0037		471.9	
8	SMC-N 60	tS	00h57m06s0	$-74d13m18$	−65.448						
	LHA 115-S 60		302.407	−42.901	647.1	u	4.8	0.0131		616.5	
9	SMC Ln 358	tS	00h59m12s2	$-75d05m19$	−65.886						
	Lin 358		302.260	−42.029	661.7	u	4.5	0.0173		627.6	
10	SMC-N 73	tS	01h04m39s1	$-75d48m24$	−66.438						
	LHA 115-N 73		301.855	−41.294	582.0	u	4.2	0.0134		561.5	
11	AX Per	tS	01h36m16s9	$+54d15m35$	40.536						
	MWC 411		129.519	−8.038	548.7	u	0.7	0.0116		372.9	
12	V741 Per	tD	01h58m49s7	$+52d53m48$	37.794						
	PK 133-08 1		133.119	−8.637	44.4	u	1.1	0.0623		37.0	
13	TT Ari	t	02h06m53s1	$+15d17m42$	2.309	d	>10k	0.3770	2.3	102833	10.8
			148.528	−43.795	392.5	d	275	0.3943	38.8	296.5	6.1
14	o Cet	t	02h19m20s7	$-02d58m27$	−15.932	d	145	0.0079	1.0	37132	10.1
			167.747	−57.982	385.4	u	2.2	0.0079		285.6	
15	LW Cas	s	02h57m20s6	$+60d37m15$	41.537	u	4.4	0.0021		25274	
	SVS 1144		137.780	1.431	558.6	u	3.0	0.0120		536.2	
16	s 32	s	04h37m45s3	$-01d19m09$	−23.170						
			197.484	−30.038	730.5	d	996	0.7551	39.0	549.1	9.1
17	S147	t	04h54m04s8	$-70d59m34$	−82.606						
			282.662	−34.971							
18	UV Aur	tS	05h21m49s0	$+32d30m44$	9.343						
	HD 34842		174.219	−2.349	460.9	u	0.7	0.0029		444.2	
19	LMC1	t	05h25m01s1	$-62d28m47$	−84.459						
			271.817	−33.766							
20	TV Col	t	05h29m25s4	$-32d49m07$	−55.952	u	2.1	0.0029		16676	
			236.791	−30.606	687.4	d	372	0.3510	28.7	511.6	7.0
21	N67	t	05h36m02s9	$-64d43m24$	−86.923						
			274.356	−32.351							
22	Sanduleak's *	t	05h45m19s7	$-71d16m10$	−85.112	u	1.1	0.0010		75807	
			281.914	−30.873	2474.0	u	2.1	0.0032		2365.6	

point.dates surveydates	offc stru	...nH .diam	..red.type .blue.type	.....mU .....mJ	.....mB .....mH	.....mV .....mK	burst.date .dist.[kpc]	refs..... .....
910121-0808		71.74			2.2c			30,
910121-0806		71.33				15.5-18		14,
		3.95						
		4.46						
930102-0102 910107-0118	25.4	6.58	M2IIIepv		8.9 2.79c	7.08-7.8 2.59c	0.34	15,30, 5,
		5.16						
930509-0512 901021-1101	6.1	5.16	B0		13.96	13.55 10.69m		28,30,
901017-1027		4.77	C			13.		17,
901015-1025		4.59	C			15.8 11.5		18,17,
901015-1023		4.41	C		17.0	11.5		18,17,
900730-0813		18.56	M5IIIe	6.67c'88	9.5-13.0 5.73m'88	9.0-12.9 5.45m'88	2.70	19,30,18,5
900730-0802		16.75	G2e	10.9m'88	10.56m'88	13.3 9.83m'88		19,30,17,
910730-0802 910118-0123	0.3	6.19						
930713-0802 910111-0121	0.4	2.44	M5:e	-1.7'80	-2.3	3.6-9.2 -2.5	0.12	31,30, 6,
920310-0311 900808-0817	4.0	92.38	AoIII		15.4-17.1 10.3	16.9 9.1		18,30,
900815-0218		5.34						
		8.61						
900830-0907		64.56	Ne(C8ep)	4.32c'88	9.8-11.1 3.06c	7.4-10.6 2.28,2.08	1.00	17,30,10,
		4.60						
920927-0930 900825-0905	18.5	2.02						
		5.17						
910218-0219 900909-1013	22.6	7.49		15.15'83	14.58	12.87		30,

seq	name.....	cij	ra.[e2000]	.....dec	....ecl	P	mlik	.prate	perr	pexpo	pxoff
	name-2.....	bur	..gal.lII.	.gal.bII.	surexpo	S	mlik	.srate	serr	sexpo	sxoff
23	MaC 2-4	s	05h47m36s0	+00d39m00	−22.753						
			204.912	−13.858	650.8	u	0.0	0.0129		492.4	
24	LMC S63	tS	05h48m44s2	−67d36m13	−88.487						
	HV 12671		277.629	−30.878	6207.0	d	14.5	0.0078		5899.0	99.4
25	WY Gem	t	06h11m56s2	+23d12m25	−0.204						
			187.914	2.257	533.7	u	0.0	0.0107		410.7	
26	SS73 1		06h48m45s3	−07d24m44	−30.260						
			219.236	−3.965	323.3	u	0.9	0.0042		297.5	
27	GH Gem	s	07h03m35s5	+12d02m19	−10.532						
	CSV 950		203.515	8.120	459.1	u	1.3	0.0065		437.6	
28	NSV 3539		07h20m04s6	−19d30m45	−41.203						
	BD-19 1821		233.496	−2.737	416.1	u	2.1	0.0056		396.1	
29	BX Mon	tS	07h25m23s9	−03d35m59	−25.300						
	HV 10446		220.040	5.884	392.7	u	0.5	0.0032		375.2	
30	MWC 560	s	07h25m51s2	−07d44m05	−29.361	u	0.9	0.0010		18895	
			223.760	4.046	534.7	u	2.6	0.0194		406.5	
31	NQ Gem		07h31m55s0	+24d30m11	2.710						
	HD 59643		194.635	19.354	452.1	u	1.4	0.0066		431.0	
32	Wray 15-157	tD	08h06m35s1	−28d31m59	−47.371						
	IRAS 08045-282		246.606	1.948	288.5	u	0.3	0.0060		260.7	
33	RX Pup	tDr	08h14m12s4	−41d42m58	−59.090	d	504	0.0448	3.8	13171	23.2
	HV 3372	bu	258.510	−3.939	539.5	d	18.0	0.0346	10.2	524.6	37.1
34	He 3-160	tS	08h24m52s8	−51d28m35	−66.587						
	Wray 15-208		267.678	−7.871	809.4	u	0.7	0.0032		767.5	
35	AS 201	tD	08h31m42s8	−27d45m32	−44.827						
	PK 249+06 1		249.078	6.969	416.1	u	0.8	0.0044		401.9	
36	WY Vel		09h21m59s2	−52d33m51	−61.924						
	HV 3655		274.142	−1.816	508.6	u	0.7	0.0047		488.5	
37	KM Vel		09h41m13s4	−49d22m42	−57.544						
	PK 274+02 1		274.188	2.577	514.2	u	0.3	0.0049		505.3	
38	He 2-38	tD	09h54m43s3	−57d18m53	−62.111	u	0.6	0.0037		22319	
	V366 Car		280.808	−2.241	33.1	u	0.0	0.0000		25.0	
39	NSV 4775		10h11m03s1	−57d48m13	−60.856	d	533	0.0253	1.9	29693	18.1
	BD-57 2768		282.857	−1.324	197.9	d	37.7	0.1123	27.6	195.0	1.3
40	He 3-404		10h21m33s9	−58d05m45	−60.046						
	Wray 15-549		284.177	−0.789	309.3	u	0.0	0.0199		227.1	
41	He 3-461	s	10h39m08s5	−51d24m12	−53.399						
			282.905	6.250	101.5	u	0.1	0.0037		96.9	
42	RT Car	s	10h44m47s1	−59d24m59	−58.769	d	10.5	0.0018	0.5	78721	122.7
	HV 107		287.442	−0.408	328.4	u	1.4	0.0193		246.7	
43	SS73 29	tS	11h08m27s5	−65d47m17	−60.827						
			292.632	−4.997	453.4	u	0.4	0.0022		435.3	
44	He 3-653	s	11h25m32s5	−59d56m32	−55.481						
	Wray 15-807		292.365	1.156	264.4	u	0.4	0.0035		255.3	
45	SY Mus	tS	11h32m10s5	−65d25m10	−58.691						
	HV 3376		294.808	−3.805	425.1	u	4.3	0.0093		406.9	

point.dates surveydates	offc stru	...nH .diam	..red.type .blue.type	.....mU .....mJ	.....mB .....mH	.....mV .....mK	burst.date .dist.[kpc]	refs..... .....
900903-0911		22.60						
900907-1217		5.67	C	12.48'83	11.60	11.3		30,
900911-0918		59.49	M2Iabpe	2.98c'83	2.09c	7.66'92 1.83		31,30,
900922-0930		57.13	M2ep		13.5	12.0		18,27,
900924-0930		11.77			12.4-14.6	14.6 9.7'74		19,30,
901005-1011		69.71	M3ep		9.5-11.5	9.5		18,
901002-1009		17.97	M4ep FOII-III	6.91c'88	9.5-13.4 5.97c	12. 5.89,5.58		18,30,
920429-0430 901002-1011	0.4	33.35						
900930-1007		5.29	C6,2/R9ev	4.05	10.0 3.33	7.4-8.0		31,30,22,
901023-1029		45.34	G			13.1 9.4		18,17,
930412-0608	0.4 w	78.43 3.70o	Mep	4.05-5.92	11.1-14.1 2.82-4.70	9.3-12.3 1.94-3.49	1972 1.00- 1.30	18,30, 7,15 2,10,
901115-1126		38.90	M7			12.5 7.5	20.00	25,17, 1,
901029-1107		14.22	G2III			11.4 9.0'74	1.26	18,30,17,12
901203-1213		128.3	M3epIb A2		8.8-10.2	13.5		22,
901205-1213		37.59		9.92'90011	7.93	15.6 6.10	3.00	18,30,6
911211-1212 901219-0117	25.0	158.6	M	6.5'83	5.29	3.7V	2.80	30, 6
920724-0728 901226-0117	0.3	189.4	M3ep OB		11.0	10.5		18,
900714-0117		178.5		8.64'80	7.64	12.5 7.00		25,30,
901226-0117		33.56				9.8 3.9		25,17,
920610-0615 901230-0118	16.5	126.3	M2Ia O	3.1'880623	10.6 3.16c	8.2-9.9 1.82		31,30,
910113-0125		42.15	G Be(pec)		13.0	13. 9.4'75		18,30,
910109-0120		83.31	Be	6.97'75	5.79	12.5 5.40		25,30,
910120-0125		64.63	M2	5.9'82	11.3-12.3 4.95	10.2-12.7 4.62	1.00	18,30, 5,

seq	name.....	cij	ra.[e2000]	.....dec	....ecl	P	mlik	.prate	perr	pexpo	pxoff
	name-2.....	bur	..gal.lII.	.gal.bII.	surexpo	S	mlik	.srate	serr	sexpo	sxoff
46	BI Cru	tD	12h23m26s4	$-62d38m16$	-52.766						
	SVS 1855		299.722	0.059	49.7	u	0.0	0.0093		43.8	
47	CQ Dra	t	12h30m07s1	$+69d12m07$	61.188	d	149	0.0084	0.9	61032	28.8
	4 Dra		125.748	47.809	951.7	d	14.4	0.0211	7.4	717.6	33.7
48	TX CVn	tS	12h44m42s2	$+36d45m49$	37.654						
	BD+37 2318		130.929	80.260	557.5	u	0.6	0.0032		528.9	
49	He 2-87	tS	12h45m47s1	$-63d00m32$	-51.418						
	PK 302-00 1		302.292	-0.144	193.3	u	0.0	0.0349		149.5	
50	He 3-828	tS	12h50m58s0	$-57d50m46$	-46.892						
	Wray 15-1022		302.870	5.026	105.1	u	0.2	0.0084		90.5	
51	SS73 38	tD	12h51m26s3	$-64d59m58$	-52.571						
	CD-64 665		302.933	-2.128	14.3		0.0	0.0000		20.6	
52	EX Hya	t	12h52m24s4	$-29d14m56$	-21.692	d	$> 10k$	5.8116	4.0	63794	5.2
	4U1249-28		303.185	33.622	433.1	u	0.2	0.0166		318.2	
53	He 3-863	tS	13h07m43s8	$-48d00m22$	-37.184						
			305.750	14.777	316.3	u	3.3	0.0175		302.7	
54	St 3-22	tS	13h14m30s6	$-58d51m52$	-46.023						
	PK 305+03 1		305.918	3.874	193.4	u	0.0	0.0349		149.5	
55	He 3-886	s	13h16m01s8	$-37d00m07$	-26.661						
	NSV 6160		308.375	25.610	295.5	u	3.8	0.0219		277.7	
56	V840 Cen		13h20m49s3	$-55d50m13$							
57	He 3-905	tS	13h30m37s2	$-57d58m17$	-44.152						
	Wray 15-1108		308.126	4.505	55.3		0.0	0.0000		38.5	
58	RW Hya	tS	13h34m18s2	$-25d22m49$	-14.449	u	1.2	0.0039		4096.4	
	MWC 412		314.994	36.486	338.2	u	0.5	0.0040		330.7	
59	He 3-916	tS	13h35m28s9	$-64d45m44$	-49.576						
	Wray 15-1123		307.608	-2.291	235.4	u	3.6	0.0200		225.8	
60	V704 Cen	s	13h54m56s1	$-58d27m18$	-42.989						
	PK 311+03 1		311.175	3.397	381.6	u	2.5	0.0217		293.9	
61	He 2-104	s	14h11m52s0	$-51d26m23$	-35.627						
	V852 Cen		315.480	9.462	281.5	u	0.0	0.0018		279.9	
62	V835 Cen	tD	14h14m09s0	$-63d25m44$	-46.243						
	NSV 6587		312.027	-2.027	444.8	u	1.6	0.0082		433.2	
63	BD-21 3873	tS	14h16m34s3	$-21d46m51$	-7.650						
			327.874	36.934	345.3	u	1.7	0.0077		326.2	
64	V748 Cen	s	14h59m34s6	$-33d25m27$	-15.727						
	CD-32 10517		331.507	22.242	311.1	u	1.5	0.0061		301.6	
65	He 2-127	tD	15h24m49s8	$-51d49m48$	-31.986						
	PK 325+04 2		325.542	4.179	398.7	u	0.4	0.0038		381.2	
66	He 3-1092	tS	15h47m10s8	$-66d29m16$	-45.115						
	PK 319-09 1		319.225	-9.349	326.7	u	1.8	0.0045		306.8	
67	He 3-1103	tS	15h48m28s4	$-44d19m00$	-23.701						
	Wray 15-1359		333.206	7.903	427.3	u	1.3	0.0091		409.8	
68	HD 330036	sD	15h51m15s8	$-48d44m54$	-27.892						
	PK 330+04 1		330.780	4.155	125.8	u	4.1	0.0314		116.1	

point.dates surveydates	offc stru	...nH .diam	..red.type .blue.type	.....mU .....mJ	.....mB .....mH	.....mV .....mK	burst.date .dist.[kpc]	refs..... .....
910123-0125		183.6	M	7.38'88111	11.0-14.0 6.17	11.0-14.0 4.7V	2.00	18,30, 6,
910404-0405 901025-1105	0.2	1.69	M3IIIa	1.36'84		4.958'92		31,30,
901203-1209		1.34	KOIII-M4 B1-B9Veq	7.43'88	9.2-11.8 6.61c	9.1-10.0 6.26		18,30,
900730-0813		159.6	M7.5			6.06	13.00	30,18, 1,
910121-0125		30.70	M6		13.5	12.5-13.5 7.1	10.00	18,17,1
900730+0813		108.6				12.5-13.8 6.1	4.20	18,29, 6,
910716-0717 910103-0118	0.1	6.10	CVint.pola			11		32,
910120-0125		12.80	K4			11.0 8.5		18,
900730-0813		37.99	M			8.5		17,
910113-0121		4.42			12.6 5.96c'72	10. 5.67		25,30,
900730+0813		40.95	K4			12.5	2.30	18,17, 1,
920130-0201 910111-0120	0.2	5.29	M2IIIep	5.73c'88	10.0-11.2 4.90c	8.1-9.6 4.70	0.60- 1.00	18,30, 1,
900730-0806		115.5	M6			12.5 7.8	30.00	18,17, 1,
900730-0813		57.23			14.3-<16 10.1'74	13. 8.39		18,30,
900730-0804		29.84		10.7'89	8.7	14.6 6.9	4.30	23,30, 6,
900804-0812		134.8	M	10.1'73	5.7	4.4 4.3V	2.80	18,30, 6,
910121-0125		7.04	G			9.6 7.2V		20, 9,
900730-0806		8.84	M Fep			11.6-13.7 8.12		18,30,
900810-0817		45.76	M7			15.6 9.5'74	14.00	23,30,18,6
900819-0827		15.97	K5	8.98'74	13.5 7.96	14. 7.67	2.10	18,30,17,1
900812-0819		20.56	M0			12.2 8.4	3.50	17, 1,
900815-0821		57.99			11.8	11.040'92 7.6		31,17,

seq	name.....	cij	ra.[e2000]	.....dec	....ecl	P	mlik	.prate	perr	pexpo	pxoff
	name-2.....	bur	..gal.lII.	.gal.bII.	surexpo	S	mlik	.srate	serr	sexpo	sxoff
69	He 2-139	tD	15h54m44s7	$-55d29m36$	-34.301	u	0.1	0.0045		11622	
	PK 326-01 1		326.914	-1.400	380.7	u	0.5	0.0039		363.4	
70	T CorB	tS	15h59m30s2	$+25d55m12$	45.275						
	MWC 413	rn	42.375	48.164	557.8	u	0.7	0.0040		551.0	
71	AG Dra	tS	16h01m41s0	$+66d48m09$	78.399	d	$> 1k$	0.8808	20.2	9100.9	43.2
	BD+67 922		100.288	40.971	1492.0	d	$> 1k$	1.1489	29.4	1425.8	7.1
72	V345 Nor		16h06m44s7	$-52d03m03$	-30.540						
	HV 8827	bu	330.507	0.043	376.0	u	1.4	0.0044		354.8	
73	Wray 16-202	tS	16h06m57s1	$-49d26m41$	-27.988						
	PK 332+01 1		332.279	1.955	350.5	u	0.5	0.0034		342.3	
74	SZ 134		16h09m12s1	$-41d40m22$	-20.300						
	Wray 15-1423		337.842	7.417	288.3	u	2.8	0.0098		283.2	
75	He 2-147	tD	16h14m00s8	$-56d59m31$	-35.132						
	V347 Nor		327.919	-4.298	370.3	u	1.5	0.0092		350.5	
76	UKS Ce-1	tS	16h15m29s3	$-22d12m16$	-0.922						
	UKS 1612-22.0		353.022	20.248	292.3	u	0.0	0.0013		294.8	
77	QS Nor		16h21m07s9	$-42d23m54$	-20.598						
	PK 338+05 2		338.936	5.356	333.1	u	0.3	0.0033		321.6	
78	Wray 15-1470	tS	16h23m21s6	$-27d40m10$	-6.005						
			350.062	15.238	376.8	u	2.0	0.0111		361.9	
79	He 2-171	tD	16h34m04s2	$-35d05m23$	-12.976						
	PK 346+08 1		346.028	8.551	324.3	u	1.9	0.0116		300.3	
80	He 3-1213	tS	16h35m15s2	$-51d42m24$	-29.357						
	Wray 15-1511		333.869	-2.815	342.6	u	2.2	0.0118		331.6	
81	He 2-173	tS	16h36m24s6	$-39d51m42$	-17.626						
	PK 342+05 1		342.772	5.011	347.9	u	0.0	0.0155		330.6	
82	HD 149407	t	16h37m20s8	$-53d46m35$	-31.346						
	CPD-53 8091		332.223	-3.936	471.8	u	0.8	0.0146		350.6	
83	He 2-176	tD	16h41m31s2	$-45d13m05$	-22.786						
	PK 339+00 1		339.394	0.745	334.0	u	1.0	0.0060		320.2	
84	He 3-1242	tS	16h44m35s5	$-62d37m13$	-39.910						
	KX TrA		326.415	-10.939	166.5	u	1.9	0.0161		164.1	
85	AS 210	tD	16h51m20s5	$-26d00m27$	-3.482						
	Wray 16-237		355.516	11.553	339.4	u	1.2	0.0054		326.9	
86	HK Sco	tS	16h54m40s8	$-30d23m04$	-7.745						
	HV 4493		352.486	8.267	333.7	u	0.0	0.0102		319.8	
87	CL Sco	tS	16h54m51s9	$-30d37m17$	-7.976						
	HV 4035		352.323	8.089	331.3	u	4.8	0.0199		318.9	
88	MaC 1-3	s	17h01m30s0	$-47d46m00$	-24.873						
			339.618	-3.528	384.1	u	1.0	0.0147		288.8	
89	V455 Sco	sS	17h07m21s8	$-34d05m14$	-11.153						
	AS 217		351.175	3.886	313.8	u	2.7	0.0132		304.1	
90	V2051 Oph	t	17h08m19s1	$-25d48m28$	-2.889	d	28.1	0.0141	4.1	3887.3	4.2
			358.010	8.624	421.4	d	7.6	0.0278		327.0	23.8
91	He 3-1341	tS	17h08m36s7	$-17d26m29$	5.451						
	NSV 8226		5.016	13.393	363.2	u	2.2	0.0110		351.6	

point.dates surveydates	offc stru	...nH .diam	..red.type .blue.type	.....mU .....mJ	.....mB .....mH	.....mV .....mK	burst.date .dist.[kpc]	refs..... .....
930309-0313 900817-0823	26.3	156.8	M	8.10'74	6.40	16.8 5.3V	5.00	18,30, 6,
900730-0804		4.67	gM3III sdBe	5.83'88	4.97	2.0-10.8 4,72	1946,1866 1.24- 1.35	31,30, 5,
920416-0416 901118-1207	4.7	3.15	K1IIpevar	7.09c'88	8.9-11.8 6.34	7.6-10.5 6.18	1.00- 1.20	31,30, 1,
900817-0825		251.1			13-<18		1985	18,14,
900817-0823		105.4	M			6.8		17,
910313-0313 900817-0823		25.99	Mep		14.0 9.98'83	12.5 9.62		18,30,
900821-0827		39.68	M8	7.06'74	5.73	15. 4.92	3.40	28,30,17,6
900812-0821		10.86	C			15.0 11.3		17,
900819-0825		39.73	Be	9.5'74	8.46	13.5-15.5 8.06		22,30,18,
900817-0823		15.14	M4e			12.0 7.8	1.70	17,18, 1,
900819-0827		22.19	M	9.52'74	7.64	6.2V	4.70	30, 6,
900823-0830		64.72	M2e		13.5	10.4 6.7	1.00	18,17, 1,
900821-0827		37.14	M	8.48'74	13.5 7.10	6.78		18,30,17,
900823-0901		40.02	B8			8		26,
900823-0830		124.2	M7			15. 5.7		28,17,
900827-0903		14.10	M6		13.1	12.4 6.20	5.00	18,30,17, 1
900823-0830		15.98	G	9.87c'88	14.0 8.08c	11.5 6.52,6.35	4.90	18,30,17,6
900823-0830		17.49	M		13.1-15.8	15. 7.9	2.80	18,17, 1,
900823-0901		19.18	M		11.2-13.9	12. 7.9	2.30	18,17, 1,
900827-0903		57.05						
900827-0903		29.98	M		12.8-<16.5	15. 5.9	5.00	18,17, 1,
920920-0921 900825-0903	0.1	21.66						
900825-0901		16.90	M2 B		13.5-16.9	12.0 7.60	2.40	18, 9, 1,

seq	name.....	cij	ra.[e2000]	.....dec	....ecl	P	mlik	.prate	perr	pexpo	pxoff
	name-2.....	bur	..gal.lII.	.gal.bII.	surexpo	S	mlik	.srate	serr	sexpo	sxoff
92	He 3-1342	tS	17h08m55s1	$-23d23m37$	-0.472						
			0.079	9.920	331.4	u	1.1	0.0059		319.5	
93	AS 221	tS	17h12m12s3	$-32d37m48$	-9.612						
	Wray 15-1637		352.952	3.934	162.9	u	0.3	0.0064		152.8	
94	PN H 2-5	tS	17h15m18s6	$-31d34m03$	-8.500						
	PK 354+04 2		354.202	4.020	131.3	u	1.4	0.0330		110.8	
95	PN Sa 3-43	s	17h17m55s7	$-30d01m44$	-6.923						
	PK 355+04 1		355.787	4.447	191.8	u	1.2	0.0063		192.6	
96	Draco C-1	t	17h19m57s6	$+57d50m05$	80.131	d	397	0.0437	3.1	21882	14.5
			86.273	34.759	1678.0	d	57.6	0.0491	7.0	1607.0	15.6
97	He 3-1383		17h20m31s7	$-33d09m48$	-10.010						
	Wray 15-1680		353.529	2.201	460.5	u	1.0	0.0153		329.7	
98	PN Th 3-7	tS	17h21m02s6	$-29d22m51$	-6.229						
	PK 356+04 3		356.708	4.261	330.1	u	0.1	0.0041		317.5	
99	PN Th 3-9	s	17h24m00s1	$-31d02m00$	-7.837						
			355.703	2.801	400.8	u	0.2	0.0088		310.2	
100	PN Th 3-17	tS	17h27m31s8	$-29d03m56$	-5.827						
	PK 357+03 3		357.764	3.266	295.4	u	0.8	0.0093		285.8	
101	PN Th 3-18	tS	17h28m26s9	$-28d38m33$	-5.393						
	PK 358+03 5		358.229	3.332	298.1	u	1.5	0.0075		286.6	
102	He 3-1410	tS	17h29m06s4	$-29d43m22$	-6.464						
	NSV 8805		357.406	2.616	312.5	u	0.0	0.0126		299.2	
103	GX 1+4	tS	17h32m02s2	$-24d45m00$	-1.465	d	20.7	0.0052	1.6	9489.5	19.0
	V2116 Oph		1.934	4.792	301.5	d	12.4	0.0321	13.0	290.8	1.1
104	PN Th 3-29		17h32m27s6	$-29d05m07$	-5.790						
	PK 358+02 3		358.341	2.355	378.4	u	1.6	0.0130		297.4	
105	PN Th 3-30	tS	17h33m43s4	$-28d07m21$	-4.816						
	PK 359+02 1		359.300	2.646	310.8	u	0.0	0.0161		297.6	
106	PN Th 3-31	tS	17h34m16s8	$-29d29m11$	-6.173						
	PK 358+01 2		358.220	1.804	321.1	u	1.1	0.0071		307.1	
107	PN M 1-21	tS	17h34m17s3	$-19d09m21$	4.148						
	PK 006+07 1		6.962	7.358	309.2	u	0.5	0.0032		297.9	
108	He 2-251		17h35m21s7	$-29d45m25$	-6.433						
	PK 358+01 3		358.119	1.460)		u	4.8	0.0144		293.4	
109	V503 Her	s	17h36m46s1	$+23d18m14$	46.587						
			47.001	26.232	669.2	u	0.8	0.0021		637.5	
110	Pt-1	tS	17h38m49s7	$-23d54m03$	-0.550						
	PK 003+03 3		3.485	3.942	332.7	u	0.0	0.0116		318.0	
111	LuSt-1	t	17h39m18s1	$-28d15m00$	-4.893	u	1.7	0.0061		9223.3	
			359.854	1.541	423.8	u	1.1	0.0199		315.0	
112	RT Ser	tS	17h39m51s9	$-11d56m37$	11.408						
	MWC 265	sn	13.896	9.971	354.7	u	3.1	0.0138		343.7	
113	AE Ara	tS	17h41m04s9	$-47d03m20$	-23.674						
	HV 5491		343.999	-8.659	175.6	u	2.6	0.0173		169.6	
114	SS73 96	tSr	17h41m28s3	$-36d47m42$	-13.417						
			352.847	-3.377	319.4	u	0.8	0.0034		313.2	

point.dates surveydates	offc stru	...nH .diam	..red.type .blue.type	.....mU .....mJ	.....mB .....mH	.....mV .....mK	burst.date .dist.[kpc]	refs..... .....
900827-0903		18.39	M2 B	8.9c'88	14.0 7.94	12.0 7.60	5.00	18,30, 1,
900827-0903		35.90	M4		17.0 8.07'74	11.0-13.1 7.49	5.00	18,30,17, 1
900830-0905		35.31	M	7.13'83	5.98	5.55		30,17,
900830-0905		40.68				7.9		17,
920401-0401 900730-0817	0.3	2.54	C1,2			17.0		17,
900830-0907		71.46	Mep			12.5		
900830-0905		42.18	M		8.55'73	14.0 8.05	10.00	21,30,17, 1
900830-0907		58.84			9.0'75	8.75		30,
900901-0907		49.09	M3		8.38'75	14. 8.18	5.00	21,30,17, 1
900901-0907		49.09	M2	9.6'74	8.38	12.6 8.03	3.50	21,30,17, 1
900901-0907		51.22	M B	9.8'74	9.08	12.5-13.1 8.41	5.00	18,30, 1,
930918-0918 900901-0907	0.0	32.09	M6III			18.7-19.4 8.1	13.00	18,17, 1,
900901-0909		64.40				13.4		21,
900903-0909		42.98	K5			13.1 9.2'74		21,30,17,
900903-0909		64.40	M5	9.23'74	8.03	13.6 7.57	8.00	21,30,17, 1
900901-0909		23.92	M2	8.77'74	14.0 7.63	14. 7.21	2.40	18,30,17, 1
					10.7'75	16.5 7.3		28,30,
900830-0907		6.97	M2p		11.1-14.4	12.5		18,
900903-0909		31.42	M1			15. 8.6		17,
920229-0301 900903-0911	17.0	53.30						
900903-0909		19.62	M A8(pec)	8.36'88	10.6-17.0 7.34	13. 6.94	1909 9.00	18,30,16, 1
900905-0911		22.05	M2 Be		11.5-13.8	11.5-13.8 6.3	1.60	18, 1,
	w	47.93 0.17r	M2 Be	8.11'75	14.0 6.85	12. 6.39	1.70	18,30, 7,17 1,

seq	name.....	cij	ra.[e2000]	.....dec	....ecl	P	mlik	.prate	perr	pexpo	pxoff
	name-2.....	bur	..gal.lII.	.gal.bII.	surexpo	S	mlik	.srate	serr	sexpo	sxoff
115	UU Ser	tS	17h42m38s4	$-15d24m40$	7.965						
	HV 8771		11.232	7.616	326.2	u	0.8	0.0071		317.0	
116	V2110 Oph	tD	17h43m32s5	$-22d45m34$	0.626						
	AS 239	rn	5.029	3.623	343.7	u	0.3	0.0038		323.0	
117	SSM 1	tS	17h43m54s8	$-36d03m24$	-12.664						
	V916 Sco	bu	353.735	-3.408	315.4	u	0.1	0.0024		302.4	
118	NSV 9601		17h44m26s2	$-02d04m47$	21.303						
	HD 161224		23.230	13.873	528.6	u	0.8	0.0055		405.0	
119	PN H 2-19		17h45m14s3	$-38d17m25$	-14.889						
	AS 241		351.959	-4.794	266.0	u	1.3	0.0045		262.7	
120	HD 161213		17h45m33s1	$-38d39m47$	-15.260						
	PK 351-05 1		351.670	-5.039	251.5	u	0.1	0.0027		247.2	
121	PN Bl 3-2	s	17h46m00s1	$-26d58m00$	-3.565						
			1.726	0.953	400.3	u	1.9	0.0166		309.7	
122	V917 Sco	tS	17h48m03s9	$-36d08m18$	-12.725						
			354.100	-4.168	273.4	u	1.1	0.0073		262.2	
123	PN Bl 3-11	s	17h48m12s1	$-28d01m00$	-4.604	u	0.0	0.0037		5895.6	
			1.081	-0.007	390.2	u	0.7	0.0083		303.6	
124	PN H 1-36	tDr	17h49m48s2	$-37d01m27$	-13.603						
	PK 353-04 1		353.515	-4.921	243.4	d	13.0	0.0745	24.4	236.7	54.5
125	RS Oph	tSr	17h50m13s2	$-06d42m27$	16.710	d	97.8	0.0106	1.5	21709	16.2
	MWC 414	rn	19.801	10.372	355.9	u	4.6	0.0155		336.2	
126	Wray 16-312	s	17h50m16s8	$-30d57m35$	-7.538						
	PK 358-01 2		358.790	-1.910	324.5	u	0.5	0.0045		306.3	
127	PN Th 4-4	s	17h50m23s8	$-19d53m45$	3.525						
	V4141 Sgr		8.312	3.732	320.6	u	1.2	0.0056		305.7	
128	AS 245	s	17h50m58s0	$-22d19m24$	1.099						
			6.289	2.379	458.0	u	1.2	0.0108		335.2	
129	PN H 2-28	tS	17h51m01s2	$-22d19m34$	1.097						
	AS 245		6.293	2.368	336.2	u	0.4	0.0024		320.7	
130	He 2-294	tS	17h51m45s4	$-32d54m53$	-9.488						
	PK 357-03 1		357.266	-3.176	292.5	u	1.9	0.0099		279.9	
131	KW Sgr		17h52m00s3	$-28d01m30$	-4.598						
	HD 316496		1.505	-0.733	322.3	u	2.5	0.0073		315.0	
132	PN Bl 3-14	tS	17h52m26s0	$-29d45m59$	-6.338						
	PK 000-01 4		0.054	-1.700	323.0	u	2.9	0.0130		309.9	
133	PN Bl 3-6	t	17h52m56s4	$-31d19m20$	-7.892						
	PK 358-02 2		358.768	-2.584	304.1	u	2.8	0.0133		292.5	
134	PN Bl L	tS	17h53m13s5	$-30d18m01$	-6.870						
	PK 359-02 1		359.680	-2.119	310.2	u	0.6	0.0046		302.7	
135	MaC 1-9	s	17h55m54s1	$-14d07m00$	9.319						
			13.986	5.503	423.0	u	0.3	0.0172		304.3	
136	AS 255	tD	17h57m08s8	$-35d15m34$	-11.822						
	MHA 363-45		355.794	-5.318	201.8	u	0.0	0.0216		192.0	
137	V2416 Sgr	tS	17h57m15s9	$-21d41m28$	1.747						
	PK 007+01 2		7.573	1.440	282.6	u	1.6	0.0078		273.6	

point.dates surveydates	offc stru	...nH .diam	..red.type .blue.type	.....mU .....mJ	.....mB .....mH	.....mV .....mK	burst.date .dist.[kpc]	refs..... .....
900903-0909		20.91	M		14.6-16.0	16. 9.1		18,17,
900905-0911		32.54	M8	9.92'80	8.41	12.-19.0 7.5V	<1980 20.00	17,30,16, 1
900905-0911		44.14	M			8.3	1967	17,14,
900903-0911		13.86	K0		10.4	9.4		18,
900905-0911		27.95		9.42'75	12. 8.28	7.77		18,30,
900905-0911		27.95	K0		10.6	9.9 9.3'74		18,30,26,
900905-0911		83.90						
900905-0911		32.84	M7			13.0 8.0		17,
930316-0316 900905-0911	26.0	149.0						
	xw	29.31 5.00r	M8		7.73 10.3'75	7.4'87	7.60	28,30, 7, 6
910302-0305	0.4 e	24.79 0.20r	M2ep Oep	7.74'88	5.3 6.98	4.3-12.5 6.73,6.59,	1967 0.60- 1.60	17,30, 7,15 1,
920304-0304 900905-0913		63.81				7.6	7.80	29, 6,
900905-0911		26.46				14.1 7.9		21,17,
900905-0913		45.00				7.5	12.00	29, 6,
900905-0913		45.00	M6	8.40		11.0 10.3?'74	9.00	17,30, 1,
900907-0913		39.50	M3			9.6'74		30,17,
920303-0303 900907-0913		97.62	M0-M4	2.72'73	11.0-13.2 1.81	11.0-13.2 5.2		31,30,
900907-0913		52.26	M6			14.4 8.7		17,
900907-0913		43.02						
900907-0913		52.26	M6	9.55'75	8.19	16.0 7.81	16.00	17,30, 1,
900907-0913		33.03						
900907-0913		26.01	K3		13.5	12.0 8.4		18,17,
900907-0913		96.70	M	6.41c'88	14.6 5.09c	13. 4.50	2.30	18,30,17, 1

seq	name.....	cij	ra.[e2000]	.....dec	....ecl	P	mlik	.prate	perr	pexpo	pxoff
	name-2.....	bur	..gal.lII.	.gal.bII.	surexpo	S	mlik	.srate	serr	sexpo	sxoff
138	PN H 2-34		17h58m28s1	$-28d33m14$	-5.115						
	PK 001-02 1		1.765	-2.228	274.6	u	1.1	0.0061		267.2	
139	He 2-325		18h01m05s9	$-26d21m26$	-2.918						
	PK 003-01 1		3.963	-1.644	277.2	u	0.0	0.0146		272.1	
140	SS73 117	tS	18h02m23s1	$-31d59m10$	-8.548						
			359.193	-4.658	198.3	u	0.3	0.0078		186.8	
141	AS 269	s	18h03m24s1	$-32d42m00$	-9.262						
			358.672	-5.192	242.4	u	0.0	0.0238		178.7	
142	PN Ap 1-8	tS	18h04m29s6	$-28d21m36$	-4.925	u	0.0	0.0020		29469	
	PK 002-03 1		2.588	-3.285	262.1	u	1.3	0.0084		252.2	
143	SS73 122	tS	18h04m41s1	$-27d09m12$	-3.718						
	IRAS 18015-270		3.663	-2.732	268.4	u	0.8	0.0072		260.1	
144	NSV 10142		18h04m45s6	$-21d51m28$	1.577	u	2.2	0.0022		21730	
	WR 107		8.291	-0.154	270.4	u	3.3	0.0095		264.7	
145	AS 270	tS	18h05m33s7	$-20d20m34$	3.090						
			9.703	0.425	275.4	u	2.4	0.0081		261.2	
146	PN H 2-38	tD	18h06m01s2	$-28d17m03$	-4.852	d	7.5	0.0018	0.6	41079	46.8
	PK 002-03 4		2.818	-3.541	259.3	d	6.6	0.0496	20.0	240.5	124.3
147	SS73 129	tS	18h07m05s7	$-29d36m25$	-6.177						
	PK 001-04 3		1.772	-4.387	228.8	u	0.0	0.0194		218.7	
148	He 3-1591	tS	18h07m32s0	$-25d53m46$	-2.468						
	NSV 10219		5.073	-2.677	274.4	u	0.4	0.0067		262.7	
149	V615 Sgr	tS	18h07m40s0	$-36d06m20$	-12.677						
	HV 7199		356.088	-7.597	139.6	u	1.0	0.0175		135.2	
150	Ve 2-57	s	18h08m22s2	$-24d33m43$	-1.136						
	NSV 10241		6.333	-2.196	285.1	u	0.5	0.0032		275.5	
151	V1148 Sgr	s	18h09m06s2	$-25d59m28$	-2.568						
	NOVA Sgr 1943	bu	5.161	-3.032	323.1	u	1.4	0.0078		252.1	
152	AS 276	tD	18h09m09s5	$-41d13m25$	-17.799						
	MHA 363-7		351.639	-10.236	137.3	u	3.3	0.0276		131.7	
153	PN Ap 1-9	tS	18h10m28s9	$-28d07m41$	-4.710						
	Wray 16-377		3.430	-4.327	225.9	u	1.0	0.0101		211.4	
154	AS 281	tS	18h10m43s8	$-27d57m50$	-4.547	u	2.8	0.0020		40730	
	Wray 16-378		3.601	-4.297	221.1	u	0.4	0.0103		211.4	
155	V2506 Sgr	tS	18h11m01s7	$-28d32m40$	-5.128						
	AS 282	bu	3.121	-4.632	213.3	u	2.3	0.0154		203.6	
156	SS73 141	tS	18h12m11s3	$-33d10m42$	-9.766						
	PK 359-07 2		359.134	-7.042	167.0	u	2.0	0.0253		158.0	
157	AS 289	tS	18h12m22s2	$-11d40m07$	11.737						
	F1-11		18.091	3.189	293.1	u	2.8	0.0104		288.4	
158	Y CrA	tS	18h14m22s9	$-42d50m30$	-19.437						
	HV 169		350.611	-11.830	153.9	u	1.7	0.0087		149.9	
159	YY Her	tS	18h14m34s1	$+20d59m18$	44.367						
	AS 297		48.144	17.243	434.0	u	0.5	0.0063		422.5	
160	V2756 Sgr	tS	18h14m34s5	$-29d49m23$	-6.424						
	AS 293		2.357	-5.919	159.7	u	0.7	0.0081		155.1	

point.dates surveydates	offc stru	...nH .diam	..red.type .blue.type	.....mU .....mJ	.....mB .....mH	.....mV .....mK	burst.date .dist.[kpc]	refs..... .....
900907-0913		45.83				9.9'75		30,
900909-0916		51.87	Mep B		12.5 9.6'74	11.5 9.1		18,30,
900909-0916		29.94	M6	8.68'75	14.0 7.57	12.5 7.07	10.00	18,30,17, 1
900909-0916		29.94		10.77'85	9.88	8.88		30,
930331-0401 900909-0916	23.0	35.58	M0 Be	9.6'75	8.3	7.9	2.60	30,18, 1,
900909-0916		34.38	M7.5 Be			12.0 6.6		17,29,18,
921003-1007 900909-0916	19.9	153.5	Be(pec		9.0-13.5 9.9'75	12. 9.0		24,30,
900909-0916		181.5	M1	7.16c'88	11.0 6.00c	12.5 5.57	0.70	18,30,17, 1
930331-0401 900909-0916	0.5	29.52	M8	8.40'75	7.57	6.67	8.10	30,17, 6,
900909-0916		30.33	K			12.5 8.0		17,
900909-0916		36.60	G Be		13.0 9.5'75	12.-13. 9.0		18,30,17,
900909-0916		13.92	M1 Be	8.94'74	13.2-14.8 7.94	12.5 7.69		18,30,
900909-0918		53.75			8.37'75	12.5 7.87		18,30,
900909-0918		36.60			8.0-<16.	<16	1943	18,15,
900909-0918		9.38	M4 B			11.5-12.5 8.1		18,
900911-0918		29.52	K4 Be		9.1'74	12.5 8.8	2.60	17,30,18, 1
930328-0406 900911-0918	0.3	27.20	M5	8.28'74	7.26	12.0 6.95	7.00	17,30, 1,
900911-0918		21.46	M		8.9'74	12. 8.42	1946	17,30,14,
900911-0918		17.90	M Be		13.0	12.5 10.5?'75		18,30,
900911-0918		66.83	M3.4 B	6.77c'88	13.0 5.57c	10.5 5.10		18,30,
900911-0918		10.38	M		12.0-13.8	12. 6.6	5.00	18,17, 1,
900914-0920		10.46	M2epvar	9.02c'88	11.1-<14 8.14c	12.5-13.5 7.90		18,30,
900911-0918		17.61	M	9.01'74	13.2-15.2 8.03	11.5 7.76	3.00	18,30,17, 1

seq	name.....	cij	ra.[e2000]	.....dec	....ecl	P	mlik	.prate	perr	pexpo	pxoff
	name-2.....	bur	..gal.lII.	.gal.bII.	surexpo	S	mlik	.srate	serr	sexpo	sxoff
161	AS 296	tS	18h15m06s4	$-00d18m59$	23.069	u	2.3	0.0013		34268	
	JP11 5251		28.480	7.931	316.4	u	0.5	0.0028		305.9	
162	HD 319167	tS	18h15m24s6	$-30d31m55$	-7.137						
	PK 001-06 1		1.812	-6.410	168.7	u	0.6	0.0119		158.1	
163	He 2-374	tS	18h15m31s0	$-21d35m24$	1.801						
	PK 009-02 1		9.732	-2.213	236.5	u	2.1	0.0189		226.9	
164	AS 295B	t	18h16m05s5	$-30d51m12$	-7.463						
	V4074 Sgr		1.594	-6.689	166.8	u	1.1	0.0174		155.9	
165	V2905 Sgr		18h17m20s5	$-28d09m45$	-4.781						
	AS 299		4.117	-5.677	177.8	u	4.1	0.0322		141.9	
166	He 3-1674	tS	18h20m19s0	$-26d22m44$	-3.020						
	Wray 15-1864		6.012	-5.432	206.6	u	0.7	0.0091		186.4	
167	AR Pav	tS	18h20m28s6	$-66d04m48$	-42.691						
	MWC 600		328.535	-21.606	121.7	u	0.9	0.0181		118.0	
168	He 2-390	tD	18h20m58s7	$-26d48m27$	-3.454						
	PK 005-05 2		5.699	-5.761	183.7	u	0.8	0.0121		172.9	
169	V3804 Sgr	tS	18h21m28s4	$-31d32m04$	-8.181						
	AS 302		1.517	-8.024	173.9	u	0.0	0.0196		163.6	
170	V443 Her	tS	18h22m07s7	$+23d27m20$	46.752						
	MWC 603		51.232	16.596	570.5	u	0.0	0.0049		547.5	
171	FR Sct		18h23m22s8	$-12d40m54$	10.640	d	6.1	0.0016	0.6	30754	102.0
	SVS 588		18.472	0.340	317.2	u	0.3	0.0032		307.5	
172	V3811 Sgr	tS	18h23m29s0	$-21d53m09$	1.442						
	PK 010-03 1		10.341	-3.985	235.9	u	0.9	0.0043		226.5	
173	AS 304	tS	18h25m26s7	$-28d35m57$	-5.284						
	CD-28 14567		4.551	-7.460	161.9	u	0.6	0.0127		150.7	
174	RY Sct		18h25m31s8	$-12d41m27$	10.608						
	MWC 295		18.710	-0.128	313.7	u	0.0	0.0059		300.3	
175	V1988 Sgr	s	18h27m58s5	$-27d37m29$	-4.336						
			5.682	-7.518	140.7	u	0.0	0.0013		139.8	
176	V1017 Sgr	tS	18h32m04s1	$-29d23m53$	-6.154						
	HV 3519	bu	4.481	-9.113	138.4	u	2.2	0.0107		135.8	
177	V2601 Sgr	tS	18h38m02s1	$-22d41m50$	0.453						
	AS 313		11.152	-7.352	318.8	u	0.5	0.0050		309.6	
178	PN Sa 3-142		18h40m25s9	$-08d44m10$	14.342						
	PK 023-01 1		23.908	-1.549	332.7	u	1.8	0.0098		322.1	
179	AS 316	tS	18h42m32s8	$-21d17m47$	1.778						
	PK 012-07 1		12.886	-7.669	292.6	u	2.2	0.0091		284.5	
180	K 3-12	s	18h44m42s1	$+06d07m00$	29.063						
			37.621	4.278	562.1	u	1.2	0.0053		424.1	
181	MWC 960	tS	18h47m55s8	$-20d05m51$	2.875	u	3.1	0.0016		40511	
	MHA 204-22		14.532	-8.273	283.9	u	0.4	0.0086		269.1	
182	AS 323		18h48m35s5	$-06d41m35$	16.218	u	2.1	0.0014		36969	
	PK 026-02 2		26.649	-2.417	346.4	u	3.9	0.0129		334.2	
183	V603 Aql	t	18h48m54s5	$+00d35m02$	23.458	d	$> 10k$	0.3090	6.2	34284	2.5
			33.163	0.830	484.2	d	388	0.3838	34.3	350.0	3.4

point.dates surveydates	offc stru	...nH .diam	..red.type .blue.type	.....mU .....mJ	.....mB .....mH	.....mV .....mK	burst.date .dist.[kpc]	refs..... .....
920307-0323 900911-0920	0.4	25.95	M5	5.79'89	13.0 4.72	10.5 4.46	1.80	18,30,17, 1
900911-0918		17.61	M3	8.92'74	13.0 7.78	12.5 7.50	3.50	18,30,17, 1
900911-0918		63.12	M	8.05c'83	14.0 6.96c	12.0 6.55		18,30,17,
900911-0918		15.83	M		8.6	11.5		18,17,
900911-0920		17.74	pec Be(pec)	8.58'75	7.32	10 7.07		22,30,18,
900914-0920		21.22	M5		12.5	12.5 7.7	8.00	18,17, 1,
900911-0918		8.06	M3III+.. Of	8.24'73	8.5-13.62 7.38	6.8-13.0 7.10	3.80-10.00	31,30, 5,
900914-0920		16.60	M		13.0 10.8'74	12 7.0V	5.20	18,30, 6,
900914-0920		14.10	M6			11.5-12.2 7.3	10.00	18, 1,
900916-0924		10.00	M3ep O	6.57c'88	5.66c	11.4-11.7 5.38		18,30,
921010-1013 900914-0920	19.5	182.3	M2.5Iabpe+ OB	3.94'73	11.7-12.5 2.67	10.46'92 2.15		31,30,
900914-0920		33.05	M			14. 8.5		17,
900914-0920		14.82	M4			11.5 7.6	5.00	17, 1,
900916-0922		202.5	O8:e.. B0ep		9.7-10.3 5.80c'73	9.1-9.7 5.48		31,30,
900916-0922		14.09	M7		12.7-15.9	13.0 2.47'69		18,30,
900916-0922		13.36	G5IIIp		6.2-14.4	14 10.58'74	1919	18,30,14,
900918-0924		17.62	M5e			15 8.0	2.30	17,18, 1,
900920-0926		55.45				9.1?'74		30,
900918-0926		17.50	M			12.0 7.8		17,
900920-0928		59.07				9.2'74		30,
930407-0414 900920-0926	10.4	19.06	M0		13.5	12.0 7.8	2.50	18,17, 1,
921013-1014 900922-0928	9.0	57.17		9.21'74	8.30	12. 7.91		18,30,
910406-0415 900922-0930	0.3	149.6						

seq	name.....	cij	ra.[e2000]	.....dec	....ecl	P	mlik	.prate	perr	pexpo	pxoff
	name-2.....	bur	..gal.lII.	.gal.bII.	surexpo	S	mlik	.srate	serr	sexpo	sxoff
184	AS 327	tS	18h53m16s7	$-24d22m57$	-1.502						
	PK 011-11 1		11.144	-11.230	308.5	u	2.7	0.0164		298.8	
185	FN Sgr	tS	18h53m54s4	$-18d59m42$	3.849						
	AS 329		16.157	-9.061	315.3	u	0.6	0.0034		302.9	
186	PN Pe 2-16	tS	18h54m10s0	$-04d38m52$	18.126						
	PK 029-02 1		29.104	-2.723	219.4	u	0.8	0.0111		201.6	
187	CM Aql	tS	19h03m35s1	$-03d03m14$	19.460						
			31.595	-4.093	384.8	u	1.1	0.0039		368.1	
188	V919 Sgr	tS	19h03m45s1	$-16d59m54$	5.598						
	AS 337		19.008	-10.312	290.8	u	4.0	0.0224		285.8	
189	AS 338	tS	19h03m46s8	$+16d26m19$	38.791						
	PK 048+04 1		48.975	4.766	583.1	u	0.5	0.0024		554.0	
190	BL Tel	s	19h06m38s2	$-51d25m03$	-28.656						
	HD 177300		345.526	-23.155	135.2	u	0.6	0.0143		129.2	
191	PN Ap 3-1	tS	19h10m36s0	$+02d49m31$	25.076						
	PK 037-02 1		37.637	-2.967	425.7	u	0.4	0.0043		412.5	
192	MaC 1-17	s	19h13m00s1	$-05d21m00$	16.892						
			30.602	-7.224	519.8	u	0.7	0.0109		375.1	
193	V352 Aql	s	19h13m30s1	$+02d18m00$	24.457						
			37.503	-3.851	560.4	u	0.0	0.0081		426.8	
194	BF Cyg	tSj	19h23m53s4	$+29d40m28$	50.981						
	MWC 315		62.928	6.697	628.7	u	0.6	0.0032		599.1	
195	CH Cyg	tSj	19h24m33s1	$+50d14m30$	70.492	d	$> 10k$	0.3323	6.5	33547	8.0
	HD 182917	rn	81.859	15.580	833.3	d	60.0	0.0595	10.4	800.1	18.5
196	SS Sge	s	19h39m07s6	$+16d42m38$	37.568	u	0.2	0.0066		6203.0	
	SVS 81	bu	53.205	-2.578	492.4	u	0.4	0.0019		470.3	
197	HM Sge	tDo	19h41m57s0	$+16d44m39$	37.457	d	956	0.0456	2.7	27416	6.0
	PK 053-03 2	sn	53.567	-3.150	553.3	d	20.1	0.0280	8.8	533.8	1.8
198	He 3-1761	tS	19h42m25s9	$-68d07m41$	-45.874						
	NSV 12264		327.675	-29.757	126.5	u	0.0	0.0284		128.8	
199	AS 360	tS	19h45m49s3	$+18d36m45$	39.074						
	QW Sge		55.650	-3.023	333.2	u	1.0	0.0087		305.4	
200	V1290 Aql	s	19h46m31s4	$+10d47m07$	31.398	u	0.2	0.0007		27310	
	ZI 1783		48.910	-7.053	513.4	u	0.0	0.0073		488.7	
201	CI Cyg	tS	19h50m12s2	$+35d41m03$	55.249						
	MWC 415		70.898	4.741	567.9	u	3.8	0.0107		543.9	
202	OX Cyg		19h54m38s9	$+39d14m57$	58.296						
	AN 108.1928		74.433	5.786	688.4	u	0.5	0.0033		652.1	
203	V1016 Cyg	tDo	19h57m05s0	$+39d49m36$	58.660	d	386	0.0140	1.0	65272	3.4
	AS 373	sn	75.173	5.678	708.5	d	21.8	0.0336		685.0	0.0
204	RR Tel	tD	20h04m18s5	$-55d43m34$	-34.493	d	$> 1k$	0.2242	10.3	9199.7	10.6
	HV 3181		342.163	-32.242	195.1	d	86.8	0.2706	41.2	189.7	14.1
205	FG Sge		20h11m56s0	$+20d20m07$	39.176						
	PK 060-07 1		60.334	-7.392	558.9	u	5.4	0.0121		536.3	
206	PU Vul	tS	20h21m13s3	$+21d34m18$	39.733	d	137	0.0042	0.5	110241	6.2
	NOVA Vul 1979	rn	62.576	-8.532	566.1	u	0.1	0.0009		547.6	

point.dates surveydates	offc stru	...nH .diam	..red.type .blue.type	.....mU .....mJ	.....mB .....mH	.....mV .....mK	burst.date .dist.[kpc]	refs..... .....
900920-0928		16.75	M		8.68c'72	11.5-12.0 8.52		18,30,17,
900922-0928		13.49	Mep	9.14'73	9.0-13.9 8.17	9.0-13.9 7.92'79	5.00	18,30, 1,
900924-0930		41.22	M5 OB		8.59'74	16.0 8.09	10.00	17,30,18, 1
900926-1002		39.13	M4	9.14c'88	13.0-16.5 8.08c	13.0-16.5 7.70		15,30,17,
900924-0930		14.73	Me		12.0-<14.2	10.5-12.5 7.2	2.10	18,17, 1,
900928-1007		35.20	M3	8.76'74	11.5 7.89	11.5 7.54	7.00	18,30, 1,
900920-0928		5.37	F8Iab		7.72-9.82	7.1-9.4 4.77		31,30,
900928-1005		48.60			9.07'74	8.50		30,
900928-1005		25.60						
900928-1007		35.67	ea			13.3-18.5 9.6?'74		15,30,
	j	21.49	M5III Bep	7.58c'90	9.3-13.4 6.65	11. 6.23	4.20	18,30,11, 5
920326-0329	0.1 ej	7.23 1.50r	M7IIIvar Be	.83'90	6.0-9.1 -.17	5.6-8.5 -0.68	0.20- 0.40	31,30, 7,10
921105-1109 901009-1017	25.2	42.61				15.	1916	19,15,
921101-1103	0.3 ew	42.61 1.50o	M	7.98'89	11-<17 6.11	11-17 4.25,4.16,	1975 0.40- 2.10	18,30, 7,16 10,
900922-0930		6.59	M3			10.4 5.6	1.40	17, 1,
901013-1019		38.90	M6	8.33c'88	11.0 7.39c	11.0 7.03	10.00	18,30,17, 1
910506-0507 901011-1017	11.4	21.16			15.-16.5	15-<16.5		15,
	b	32.83	Bep+.. Bep	5.76c'88	9.9-13.1 4.79c	9.6-12.0 4.48	1.70	31,30, 8, 5
901023-1103		25.58	M2..4		14.8-16.2	15.5		18,22,
921118-1119	0.8 we	25.77 0.40o	M6	6.98'88	10.5-17.5 5.57	12.5 4.33,5.20,	1964 2.20- 3.30	18,30, 7,16 10,
930327-0330 900930-1007	0.6	4.39	M F5epv		6.5-16.5	14 3.6V	1944 2.50- 2.60	18,30,16,10
901021-1027		25.67	B4-K2pec	6.99'90	9.45-13.7 6.65	8.1-12.3 6.49		31,30,
921109-1112 901023-1101	0.4	16.00	M4-5 F8	7.71'82	8.5-16 7.2	11 5.93	1978	18,30,13,

seq	name.....	cij	ra.[e2000]	.....dec	....ecl	P	mlik	.prate	perr	pexpo	pxoff
	name-2.....	bur	..gal.lII.	.gal.bII.	surexpo	S	mlik	.srate	serr	sexpo	sxoff
207	He 2-467	tS	20h35m57s3	$+20d11m33$	37.363						
	LT Del		63.399	-12.150	563.7	u	2.1	0.0079		539.2	
208	He 2-468	tS	20h41m18s9	$+34d44m52$	50.543						
	PK 075-04 1		75.943	-4.441	692.1	u	0.9	0.0043		665.3	
209	ER Del	t	20h42m46s7	$+08d40m58$	25.890						
			54.458	-19.994	650.1	u	1.3	0.0059		492.7	
210	V1329 Cyg	tS	20h51m01s2	$+35d34m54$	50.479						
	HBV 475	bu	77.836	-5.477	684.9	u	1.4	0.0070		659.5	
211	Hen 1924	tS	21h00m06s3	$-42d38m50$	-24.506	d	694	0.0584	3.2	27225	8.1
	CD-43 14304		358.654	-41.104	379.4	d	44.7	0.1057	20.6	364.8	14.9
212	V407 Cyg	t	21h02m11s7	$+45d46m28$	58.404						
	AS 453		86.986	-0.487	724.6	u	0.7	0.0030		695.5	
213	S 190	s	21h41m45s0	$+02d43m52$	15.611						
			58.417	-35.433	486.5	u	0.6	0.0140		364.2	
214	AG Peg	tSr	21h51m02s0	$+12d37m31$	24.055	d	>1k	0.0694	3.5	24568	6.2
	MWC 379	sn	69.278	-30.887	322.7	d	24.3	0.0564	16.5	305.6	14.7
215	W Cep		22h36m27s8	$+58d25m35$	58.861						
	HD 214369		106.024	0.057	538.0	u	0.0	0.0056		512.2	
216	Z And	tS	23h33m40s0	$+48d49m06$	46.100	d	17.9	0.0019	0.5	40305	10.1
	MWC 416		109.980	-12.088	432.6	d	6.3	0.0187	9.5	411.5	43.7
217	R Aqr	tSj	23h43m49s5	$-15d17m02$	-12.403						
	MWC 400		66.519	-70.325	328.7	d	57.1	0.1284	23.2	309.5	6.1

point.dates surveydates	offc stru	...nH .diam	..red.type .blue.type	.....mU .....mJ	.....mB .....mH	.....mV .....mK	burst.date .dist.[kpc]	refs..... .....
901027-1105		9.94	G5		13.1-14.1 9.874	13 9.36		18,30,
901105-1113		48.54	M		8.25	7.96		30,17,
901025-1103		9.32						
901109-1117		30.57	M5II	8.88'88	12.1-18 7.27c	12.6-14.0 6.87	1969	18,30,16,
930408-0408 901015-1021	0.3	3.82	K3			10.0 7.6	1.20	1,
901118-1129		100.7	Mep	4.74'90	13.3-<17.0 3.64	11.5-15 2.90		18,30,17,
901107-1115		5.12						
930608-0610	0.3 e	6.40 20.0o	M1-3,II-II WN6	5.03-5.05	4.15-4.18	6.0-9.4 3.84-3.89	1857 0.60- 1.00	31,30, 7,16 3,
901228-0118		79.82	K0ep-M2epI O			6.9-8.9 2.3		31,30,
930104-0109 901230-0118	0.2	14.74	M2III B1eq	6.13'88	8.0-12.4 5.24c	7.8-11.3 4.95	1.20	15,30, 5,
	e?j	1.70 15.5o	M5-M8.5III pec	0.18-1.23	-0.80-0.14	5.8-12.4 -1.32–0.5	0.24- 0.33	15,30, 7, 4

X-Ray Properties of Symbiotic Stars: I. The Supersoft Symbiotic Novae RR Tel and SMC3 (= RX J0048.4–7332)

U. Mürset[1], S. Jordan[2], B. Wolff[2]

[1] Institut für Astronomie, ETH-Zentrum, CH-8092 Zürich, Switzerland
[2] Institut für Astronomie und Astrophysik, Universität Kiel, 24098 Kiel, Germany

Abstract. We searched the ROSAT archive for pointed PSPC observations covering positions of symbiotic stars. 16 systems are detected. We find three distinct types of energy distributions, one of which is supersoft. This class consists of seven objects, among them two symbiotic novae, RR Tel and SMC3, which are discussed in more detail in this paper. The supersoft emission is produced by photospheric emission from the hot star. For RR Tel the ROSAT and IUE observations are simultaneously reproduced with a white dwarf type atmosphere with $T_{\rm eff} = 142\,000$ K. SMC3 can only be fitted with a WR-type atmosphere with considerable mass loss ($\dot{M} \sim 10^{-5} {\rm M}_\odot/{\rm yr}$), and a temperature in excess of $T_{\rm eff} \gtrsim 260\,000$ K.

1 Introduction

Some supersoft sources have been identified as symbiotic stars. Symbiotics are a class of interacting binaries with about 150 confirmed members. The stellar components are usually a RGB or AGB star and a very hot ($T_{\rm eff} \sim 10^5$ K) white dwarf. The hot star radiatively ionizes the surrounding gas in the system, which possibly originates from the wind of the cool star. The optical spectrum is composite, with emission lines from the ionization nebula superimposed on the continuum of the red giant. The UV is dominated by nebular emission, but towards short wavelengths the contribution from the hot star increases and becomes dominant at the short wavelength end of the IUE window. For the X-ray range either supersoft photospheric emission from the hot star can be expected, or harder radiation from shocks in the gas streams.

With EINSTEIN and EXOSAT, a total of 6 symbiotic objects were detected (Allen 1981, Anderson et al. 1981, Willson et al. 1984, Kwok & Leahy 1984, Piro et al. 1985, Viotti et al. 1987, Leahy & Taylor 1987). Bickert et al. (1993) reported 14 objects to be detected in the ROSAT all-sky-survey. Since the completion of that survey, several objects were recorded during pointed observations and hidden in the ROSAT archive. In many cases the symbiotic stars were not the very target of the observation, but accidently covered by the 2° PSPC field centered on another object. In Jordan et al. (1994), Mürset et al. (1995), and

Jordan et al. (1996) we explored the interpretation possibilities of such pointed observations.

In this Paper we summarize work on the two supersoft symbiotic novae RR Tel and SMC3, and we give first results from a search for further supersoft symbiotic sources.

2 Symbiotic Stars in the ROSAT Archive

We systematically searched in the ROSAT archive for symbiotic stars. We found 30 objects situated in fields covered by pointed PSPC observations; 16 of them were in fact detected with a significant count rate (see Table 1). Details will be given in Paper II (Mürset et al. 1996b).

Table 1. Symbiotic stars detected on pointed PSPC observations.

Star	Date	Count rate $[10^{-2}\,s^{-1}]$	Type
EG And	July 1991	0.8 ± 0.3	β
SMC3	April 1992	20.4 ± 0.4	α
Ln358	Oct – Nov 1992	2.9 ± 0.2	α
RX Pup	April – June 1993	6.0 ± 0.6	β
AG Dra	1992/1993	$92 \ldots 114 \pm 3.0$	α
Draco C–1	April 1992	5.3 ± 0.6	α
GX 1+4	Sept 1993	0.6 ± 0.4	γ
Hen1591	Sept 1993	1.4 ± 0.6	γ
CH Cyg	March 1992	37.2 ± 0.9	β
HM Sge	Nov 1992	4.5 ± 0.4	β
V1016 Cyg	Nov 1992	1.2 ± 0.3	β
RR Tel	April 1992	18.3 ± 0.8	α
PU Vul	Nov 1992	0.4 ± 0.1	β
CD−43.14304	April – Oct 1993	9.1 ± 0.4	α
AG Peg	June 1993	6.7 ± 0.5	β
R Aqr	Dec 1992	4.1 ± 0.3	α

not detected: SMC2, RAW1691, BE191, N67, Sanduleak's star, MWC 560, He2–38, RW Hya, Ap1–8, H2–38, Ap1–9, AS281, MWC 960, Z And

The extracted pulse height distributions can be divided into three distinct groups (cf. Fig. 1):

- α: supersoft spectra. The two symbiotic novae RR Tel and SMC3 are typical members of this group (Jordan et al. 1994, 1996).
- β: objects with a harder pulse height distribution that typically peaks at about 0.8 keV. AG Peg (Mürset et al. 1995) may serve as a prototype.
- γ: relatively hard X-ray sources like GX1+4. In fact, GX1+4 has the hardest spectrum of all known X-ray binaries (Predehl et al. 1995).

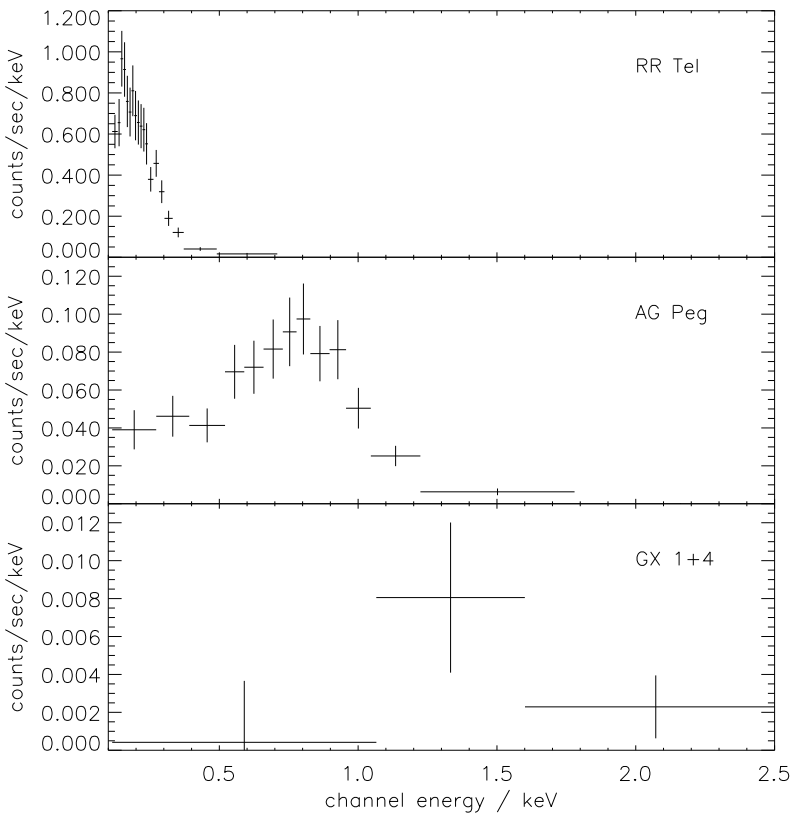

Fig. 1. Observed PSPC pulse height distributions for RR Tel (type α, Jordan et al. 1994), AG Peg (type β, Mürset et al. 1995), and GX1+4 (type γ, Predehl et al. 1995).

So far, the three X-ray types of symbiotic stars are a mere observational discovery. They become a meaningful classification scheme if they are related to physical parameters of the system. Indeed, a physical interpretation of the $\alpha/\beta/\gamma$–system appears well possible:

- α: a supersoft spectrum is expected from those symbiotic systems which contain particularly hot white dwarfs. In these cases the photospheres produce photons hard enough ($h\nu \approx 0.2$ keV) to leak into the ROSAT window.
- β: The classical model of a symbiotic nebula consists of the ionized section of the wind that flows radially away from the cool star. However, in several cases there is now clear evidence that the hot star loses mass as well. In AG Peg, for instance, N v λ1240 displays P Cyg profiles (Nussbaumer et al. 1995) which can be modelled with a wind of $v_\infty = 950$ km/s and $\dot{M} = 10^{-6.7}\,\mathrm{M}_\odot/\mathrm{yr}$ (Schmutz 1996). If the hot star sheds a substantial wind, the shock region where both winds collide is expected to have a temperature of several million

K. Mürset et al. (1995) have shown that the β–type X-ray emission of AG Peg indeed matches the theoretical predictions for the colliding wind scenario. β–type plasma emission will be analyzed in Paper II.

γ: GX1+4, which is one of the two γ–type objects, hosts a pulsar as the hot component (e.g. Davidsen et al. 1977). We may speculate that this is also the case for the other γ–type object, Hen1591.

The $\alpha/\beta/\gamma$–classification, thus, mirrors basic properties (temperature, mass-loss, white dwarf/neutron star) of the hot star. It reminds us of the infrared classes "s" and "d" (Webster & Allen 1975) which mainly correspond to basic parameters of the cool star.

A weak X-ray component of type β was detected in RR Tel which is an object of type α. From this we learn that the different emission sources do not necessarily exclude each other mutually. The classification of an object simply mirrors the relative strengths of the components.

Out of the 16 detections, 7 are supersoft (type α). For the galaxy the ratio known : observed : detected : supersoft is 150:22:13:4, whereas it is 13:8:3:3 for the extragalactic symbiotics. The surprisingly high fraction of detections of extragalactic supersoft symbiotics is partly due to the comparably long exposure times on SMC fields, but it also shows the influence of the interstellar extinction: The galactic symbiotic stars are concentrated towards the center of the Milky Way (Kenyon 1986), and many of them are strongly reddened.

3 A Model for the Supersoft Symbiotic Stars

3.1 What Can We Learn from the Supersoft X-Rays?

Supersoft X-ray data have the potential to crucially improve our understanding of the hot stars in symbiotic systems:

- It is noteworthy that the X-rays directly originate from the hot star. In other regimes of the spectrum the nebula or the cool star are much brighter than the hot star. The hot star can then only be investigated indirectly, e.g. by modelling the emission nebula with the properties of the hot star as model parameters. Indirect methods can certainly yield correct results, but at a lower level of confidence than direct observations. In the case of RR Tel Jordan et al. (1994) find similar parameters as Mürset & Nussbaumer (1994) guessed from the UV alone. On the other hand, the ROSAT based results of Jordan et al. (1996) for SMC3 strongly differ from the UV investigation by Vogel & Morgan (1994).
- The ROSAT window is even that part of the stellar spectrum which, due to the presence of ionization edges, depends most sensitively on the temperature and the chemical composition. The determination of the chemical composition of the hot star is certainly beyond the possibilities of IUE data alone.

Table 2. Solutions for RR Tel and SMC3

Parameter	RR Tel	SMC3
Type of atmosphere	hydrostatic	wind model
Elemental composition	solar	$C/He > 2 \cdot 10^{-4}$
$T_{\rm eff}$ [K]	142 000	$> 260\,000$
L [$L_\odot$]	3500	12 000
R [$R_\odot$]	0.1	< 0.05
$\log g$ [cgs]	6.5	—
$\frac{\dot{M}}{v_\infty}$ $\left[\frac{M_\odot/yr}{km/s}\right]$	—	$\sim 10^{-8}$
$N_{\rm H}$ [cm^{-2}]	$2 \cdot 10^{20}$	$9 \cdot 10^{20}$

It would, however, be wrong to base an analysis solely on X-ray data. These show an extreme end of the hot star's spectrum, and in addition the spectral resolution of the PSPC is not satisfactory. A reliable result is obtained by *simultaneously* fitting the ROSAT observations, the UV continuum (stellar + nebular) and crucial emission lines.

This was done by Jordan et al. (1994) for RR Tel and by Jordan et al. (1996) for SMC3. First, they computed a grid of model spectra appropriate for very hot stars. Then the nebular emission was calculated with a photo-ionization code. The resulting stellar + nebular emission was requested to match the ROSAT and IUE data. The stellar radius, the size of the nebula and the interstellar absorption column enter the models as additional fit parameters. Table 3.1 summarizes the solutions for the hot stars.

3.2 RR Tel

During the first decades of this century, in RR Tel the Mira type variations of the cool component were observed (Mayall 1949), and no signatures of a compact companion showed up. In 1944, the outburst started with a 7 mag brightness rise to $M_V = -5$. In the next few years, the object was wrapped into an expanded photosphere ($R \approx 100\ R_\odot$, Mürset & Nussbaumer 1994). Then, the object shrank and turned hotter, exciting low ionization emission lines in the surrounding gas. During the transition phase, strong WN-type wind features were observed by Thackeray & Webster (1974). After that, RR Tel has been smoothly evolving to higher and higher temperatures, as could be seen from the increasing ionization (e.g. Thackeray 1977). Presently, the largest observed ionization potential is that of [Mg VI]. The light curve and ionization records can be found in Mürset & Nussbaumer (1994).

A hydrostatic, white dwarf-type model atmosphere with solar elemental composition and a temperature of $T_{\rm eff} = 142\,000$ K is a possible solution to the present data (Jordan et al. 1994). Jordan et al. did not really exploit the phase space of possible chemical compositions of the atmosphere. However, we belief that the temperatures and luminosities which could possibly be derived with other abundances would not differ too much.

3.3 SMC3

SMC3 (= RX J0048.4–7332) has been in outburst since 1981 (Morgan 1992). Few is, however, known about its further history. The overall spectrum of SMC3 is remarkable. The optical spectrum (Morgan 1992, Mürset et al. 1996a) reveals nebular ionization that is unusually high for a symbiotic (Fe^{+9}). It proves that the hot star emits a significant rate of photons harder than $h\nu > 235$ eV. On the other hand, the UV spectrum (Vogel & Morgan 1994) is typical for a system with rather moderate excitation. Finally, the PSPC count rate (Kahabka et al. 1994) is higher than the count rate of RR Tel, despite of the 20 times larger distance! In summary, the spectrum looks confusing at first sight and provides a challenge to models of symbiotic stars.

Using plane-parallel, hydrostatic model atmospheres, Jordan et al. (1996) could not find a solution fitting all data consistently. It turned out that every atmosphere that is hot and luminous enough to reproduce the X-ray observations is at the same time too bright in the EUV range between the He II ionization edge and the ROSAT range leading to a brighter emission nebula than observed. The situation is different with WR-type atmosphere models. If the mass loss is sufficiently strong the wind is opaque to the emission in this spectral region. The mass loss can be adjusted to yield the observed nebular He II emission. Figure 2 shows WR-type models that differ slightly in mass loss. In this manner Jordan et al. derived a mass loss of several times 10^{-6} $M_\odot$/yr. Figure 3 displays fits to the ROSAT pulse height distribution. In order to reproduce the X-rays $T_{\rm eff} \gtrsim 260\,000$ K is required (Fig. 4 of Jordan et al. 1996). No upper limit can be specified, because with increasing temperature the energy distribution degenerates to a common shape.

4 Concluding Remarks

- The use of multi-wavelength data (optical+UV+X-ray) is extremely important for the analysis of the hot components in symbiotic systems.
- We further emphasize that sophisticated non-LTE atmospheres have to be used. Tests with black body models clearly led to wrong results.
- Accretion onto the hot components of symbiotic systems should not be adopted as self-evident; some objects lose mass at least episodically. As SMC3 shows, the mass-loss rates can be extremely high. May be, simultaneous accretion and mass-loss is possible.

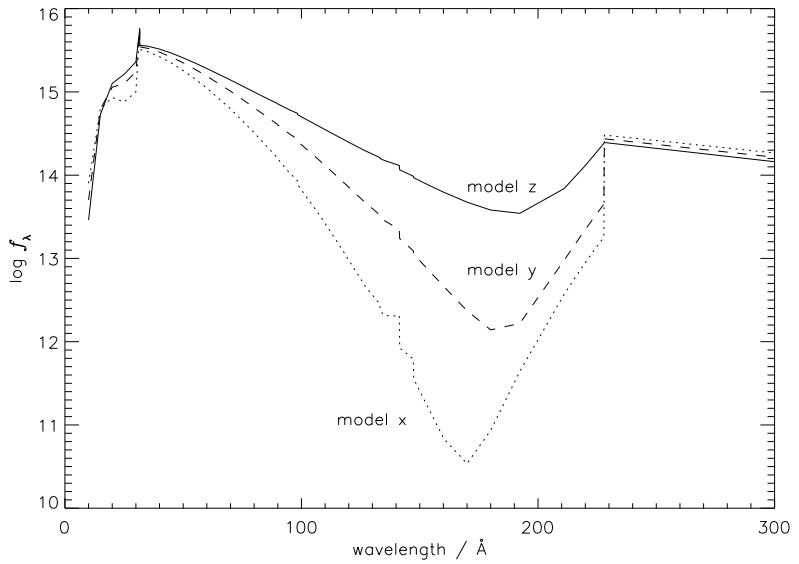

Fig. 2. Relative energy distribution of three WR-type models with approximately the same effective temperature of $T_{\rm eff}$= 300 kK, but differing in the mass loss rate (models x, y, z: $M_{\underline{x}}$= $10^{-5.1}, 10^{-5.2}, 10^{-5.3}$ $M_\odot$/yr.).

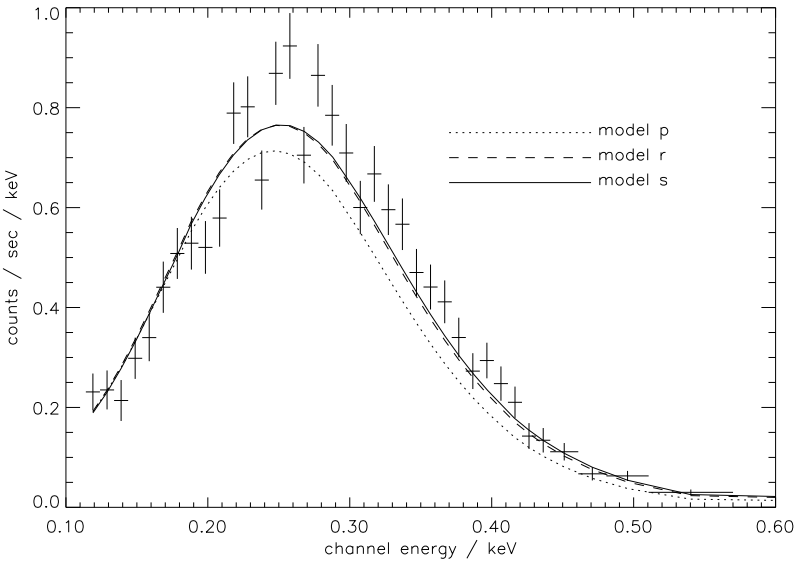

Fig. 3. Comparison of the observed PHD of SMC3 with three Wolf-Rayet type models with $T_{\rm eff}$ = 220 kK (model p), 309 kK (r), and 354 kK (s). The predicted flux from model p is not hard enough to reproduce the observation, while the two hotter models (r) and (s) lead to relatively good fit to the data. The specific parameters of the models are listed in Table 2 of Jordan et al. (1996)

- The luminosities are well below the Eddington limit.
- The wind of SMC3 contains some carbon. The matter is therefore not completely CNO processed, or carbon is admixed from outside. In this respect, SMC3 differs from the galactic symbiotic nova AG Peg which exhibits a strong carbon deficiency (Schmutz 1996).

Acknowledgement: We thank Werner Schmutz for helpful comments. Work on ROSAT data in Kiel was supported by DARA grant 50 OR 94091.

References

Allen D.A., 1981, MNRAS 197, 739
Anderson C.M., Cassinelli J.P., Sanders W.T., 1981, ApJ 247, L127
Bickert K.F., Stencel R.E., Luthardt R., 1993, in: Planetary Nebulae, IAU Symp. 155, eds. R. Weinberger & A. Acker, p. 405
Davidsen A., Malina R., Bowyer S., 1977, ApJ 211, 866
Jordan S., Mürset U., Werner K., 1994, A&A 283, 475
Jordan S., Schmutz W., Wolff B., Werner K., Mürset U., 1996, A&A (in press)
Kahabka P., Pietsch W., Hasinger G., 1994, A&A 288, 538
Kenyon S.J., 1986, The symbiotic stars, Cambridge University Press
Kwok S., Leahy D.A., 1984, ApJ 283, 675
Leahy D.A., Taylor A.R., 1987, A&A 176, 262
Mayall M.W., 1949, Harv. Bull. 919, 15
Morgan D.H., 1992, MNRAS 258, 639
Mürset U., Nussbaumer H., 1994, A&A 282, 586
Mürset U., Jordan S., Walder R., 1995, A&A 297, L87
Mürset U., Schild H., Vogel M., 1996a, A&A (in press)
Mürset U., Wolff B., Jordan S., 1996b (in prep.) (Paper II)
Nussbaumer H., Schmutz W., Vogel M., 1995, A&A 293, L13
Predehl P., Friedrich S., Staubert R., 1995, A&A 294, L33
Piro L., Cassatella A., Spinoglio L., Viotti R., Altamore A., 1985, IAU Circ. 4082
Schmutz W., 1996, in: Science with the Hubble Space Telescope II, eds. P. Benvenuti, F.D. Macchetto, E.J. Schreier (in press)
Thackeray A.D., 1977, Mem. R. Soc. 83, 1
Thackeray A.D., Webster B.L., 1974, MNRAS 168, 101
Viotti R., Piro L., Friedjung M., Cassatella A., 1987, ApJ 319, L7
Vogel M., Morgan D.H., 1994, A&A 288, 842
Webster B.L., Allen D.A., 1975, MNRAS 171, 171
Willson L.A., Wallerstein G., Brugel E.W., Stencel R.E., 1984, A&A 133, 154

Multiwavelength Observations of the Symbiotic Star AG Dra During 1979–1995

R. Viotti[1], R. González-Riestra[2], F. Montagni[3], J. Mattei[4], M. Maesano[3], J. Greiner[5], M. Friedjung[6], A. Altamore[7]

[1] Istituto di Astrofisica Spaziale, CNR, Via Fermi 21, I-00044 Frascati (Roma)
[2] IUE Observatory, ESA, P.O. Box 50727, SP-28080 Madrid
[3] Istituto Astronomico, Università La Sapienza, Via Lancisi 29, I-00161 Roma
[4] American Association of Variable Star Observers, 25 Birch Street, Cambridge, MA 02138
[5] Max-Planck-Institut für Extraterrestrische Physik, D-85740 Garching
[6] Institut d'Astrophysique, CNRS, 98bis Boulevard Arago, F-75014 Paris
[7] Dip. Fisica, Università Roma III, Via della Vasca Navale 84, I-00146 Roma

Abstract. Since 1980 the high velocity symbiotic system AG Dra has undergone three phases of activity (or "outbursts") which were extensively observed in optical, ultraviolet and X-ray bands. We describe the historical light curve of the star, and summarize 17 years of UV monitoring with the IUE satellite.

1 Introduction

The category of symbiotic stars includes some two hundred objects whose main features are: (i) the light curve, characterized by a number of "outbursts", and (ii) the composite spectrum. The latter one generally arises from the emission of a binary system composed by a late–type giant or bright giant star, and an evolved hot dwarf companion, whose radiation ionizes an extended circumstellar nebula filled in by the cool star's wind, and by some kinds of "ejecta" from the dwarf companion. The typical time scale of the variations is up to many years, which makes possible the extensive multiwavelength monitoring of a number of "representative" objects. In this regard AG Dra has been in the last years the best studied symbiotic object (and one of the best studied cataclysmic–type variables) from the optical to the ultraviolet and to X-rays, and the amount of observational data so far collected might give important clues for understanding the physics of the *cataclysmic phenomenon*.

AG Dra is a high–velocity (–148 km s^{-1}), high–galactic latitude (bII=+41°) symbiotic system, known since the earlier HEAO–2 observations for being an intense soft–X ray source (Anderson et al. 1981). The higher sensitivity at lower energies allowed the EXOSAT and ROSAT satellites to disclose the supersoft nature of the source (Piro et al. 1985, Bickert et al. 1996, Greiner et al. 1996). AG Dra is a photometric and spectroscopic binary (T=$\sim$554^d, Meinunger 1979, Mikolajewska et al. 1995), with a luminous K–star primary and a hot ($\sim$10^5 K) dwarf companion which is a source of an intense UV radiation producing a rich

emission line spectrum, and a strong UV continuum. The larger amplitude of the variation in the U–band, and the broadness of the minimum as described by Meinunger (1979) imply that the occulted region is an extended H II region in between the two stars, most probably the ionized cool star's wind. The system distance is so far unknown mainly because of the uncertainty on the luminosity class of the red component – e.g. III according to Viotti et al. (1983), Ib according to Huang et al. (1994). The classification is difficult because of the lower metallicity of the star, and of the non-negligible nebular contribution to the stellar continuum also in the longer wavelengths (as discussed below), which both should significantly affect the photospheric line ratio. Of special importance is the low interstellar absorption towards AG Dra (E_{B-V}=0.06, Viotti et al. 1983), which makes it an ideal target for far–UV and soft X-ray observations.

The most spectacular feature of AG Dra is the fact that during the last 16 years the star underwent many different phases of activity, which has given us the opportunity to study for the first time, and repeatedly, the outburst of a symbiotic system at UV and X-ray wavelengths.

The first "major" active phase of 1980–1983 was monitored with IUE, and the results were described by Viotti et al. (1984). No X-ray observation was made during the 1980 outburst because of a failure of the power supply of the HEAO–2 IPC detector. The second "minor" active phase of 1985–1986 was observed with IUE and EXOSAT, and was described by Viotti et al. (1995) and Mikolajewska et al. (1995). Viotti et al. found a marked anticorrelation of the UV and X-ray light curves, with a large fading of the X-ray source during the two light maxima, while the UV flux largely increased. We also noted that no eclipse of the X-ray source occurred on 4 November 1985, at orbital phase 0.49 according to Meinunger's (1979) ephemeris.

For the most recent 1994–1995 "major" active phase, a campaign of coordinated optical, ultraviolet, and X-ray observations was organized, which was based on numerous target of opportunity observations with ROSAT and IUE. The results of the campaign are for the first time presented in this Workshop. In the following we shall describe the IUE observations, and the optical light curve from the AAVSO databank and from BVRI photometry. We also recall that coordinated optical spectroscopy was obtained at the Observatoire de Haute Provence, and at the Padova-Asiago and Bologna-Loiano Observatories. The ROSAT X-ray data and their model implication are discussed by Greiner et al. (1996).

2 The Visual Light Curve

Photometrically, AG Dra is a variable star which is normally at minimum with V_{min}=9.8–10.0 (star's *quiescent phase*). Erratically, AG Dra undergoes 1–2 mag light maxima, or "outbursts" at time intervals from one to many years (*active phases*). Robinson (1966) recorded 11 outbursts between 1890 and 1966, and found that in many cases a second maximum occurred after 250–500 days. Iijima

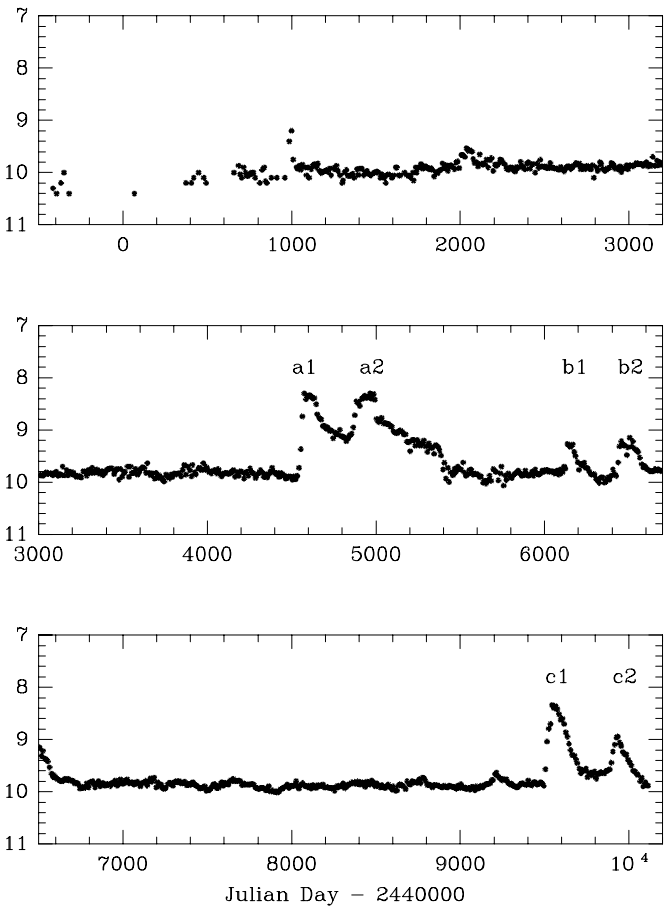

Fig. 1. The visual light curve of AG Dra from 1967 to 1995 (from AAVSO). The three most recent active phases are marked.

et al. (1987) noted that since 1935 the main outbursts repeated with an apparent periodicity of about 15 years, corresponding to nearly exactly 10 orbital periods.

Figure 1 gives the AAVSO light curve of AG Dra during 1967–1995. As shown in the figure, during the last three decades, the star has been in quiescence during 1967–1980, 1983–1985, and 1986–1994. In this period six light maxima have been recorded which can be grouped into three 1 year–splitted twin peaks ("primary" and "secondary" outbursts): November 1980–August 1981 ($a1$ and $a2$), March 1985–January 1986 ($b1$ and $b2$), and June 1994–July 1995 ($c1$ and $c2$). As concerns the two "major" active phases (1980–82 and 1994–95), the timelag was of about 4961^d, corresponding to 8.96 554^d–periods (or to 9.00 551.2^d–periods), which seems to confirm the existence of a relation between the recurrence time of the active phases and the orbital period.

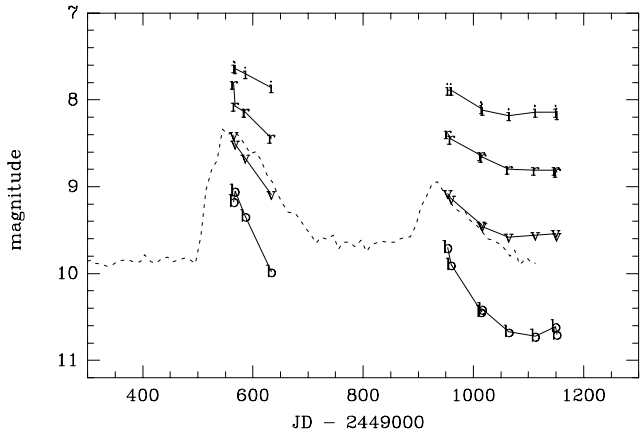

Fig. 2. The four-colour photometry of AG Dra during 1994-1995 (BVRI, from bottom to top). The dotted line is the AAVSO visual light curve.

The four–colour photometry obtained at the Greve (Firenze, Italy) and Vallinfreda (Roma) is shown in Figure 2. It appears that AG Dra largely varied in all the colours with an amplitude which is larger at the shorter wavelengths. This behaviour resembles that of AG Dra in quiescence during the orbital motion as described by Meinunger (1979). In both cases the effect is due to the larger contribution of the (variable) nebular emission towards shorter wavelengths. This shows that the *optical* outburst is the direct result of the increased volume of the ionized nebula.

3 Spectral Variation in the Ultraviolet

AG Dra has been monitored in the UV by the IUE satellite since 1979. This has given the unique opportunity to follow all the recent six "outbursts", and to analyse the behaviour of the nebular and hot dwarf's emission during different activity phases (e.g. Viotti et al. 1984, Lutz et al. 1987, Kafatos et al. 1993). It should also allow to enlighten the main features of the activity phases, which is fundamental for a correct modeling of the phenomenon. The variation of the UV continuum and emission line fluxes in the three phases of *activity* is shown in Figure 3. For the continuum we have chosen the far–UV (at 1340 Å) and near–UV (at 2860 Å) regions, which are less affected by the line emission, and where the dominant contribution is from the hot star (Rayleigh-Jeans black-body tail), and from the ionized nebula (Balmer continuum), respectively.

Fig. 3 shows that the "primary" outbursts were accompained by an increase of the UV continuum and line flux, with an amplitude tyically much larger than that in the optical region. The large increase in the N v and He II lines is an indication of a marked increase of the flux of 54–77 eV photons at the time of the outburst. The $\mathrm{He\,II}_{1640A}/\mathrm{F}_{1340A}$ flux ratio, which is a measure of the hot

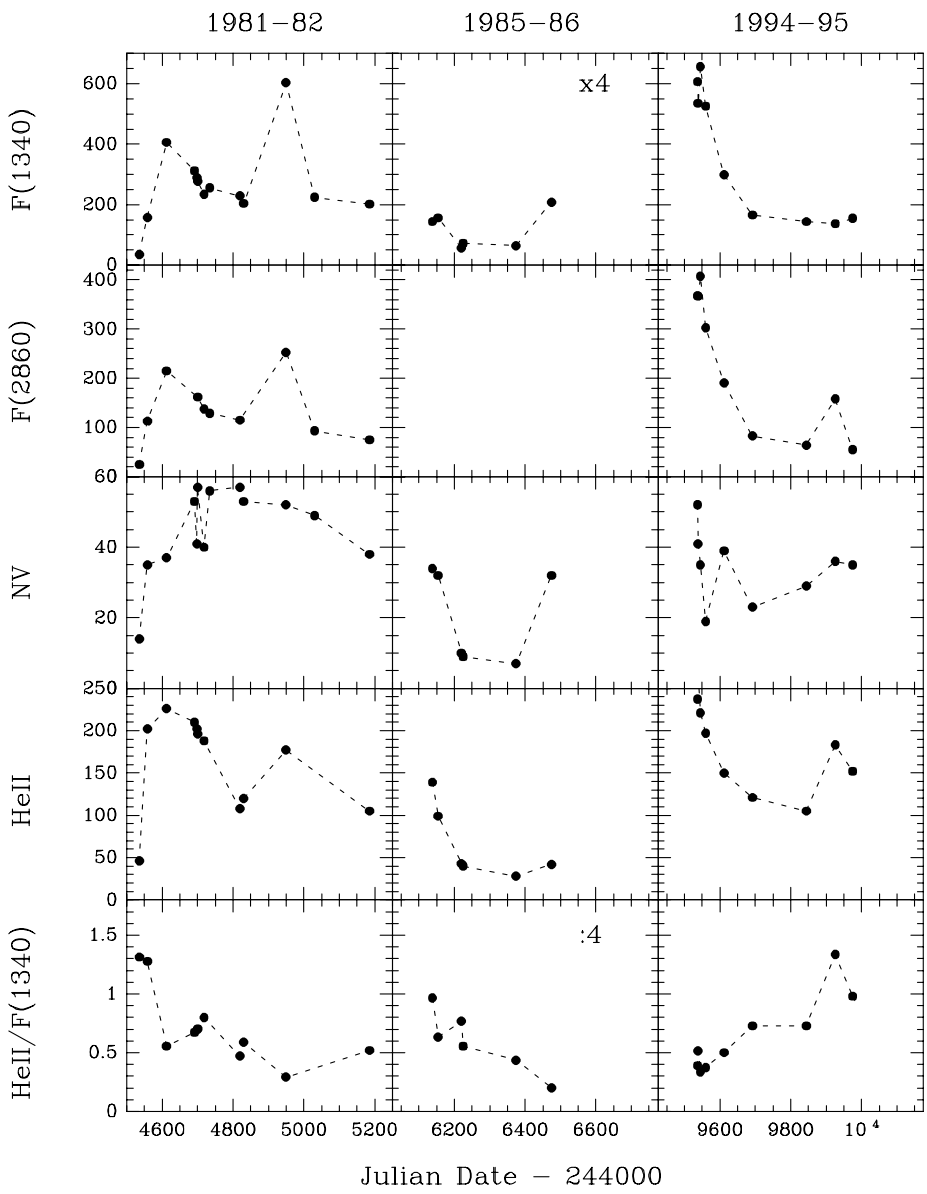

Fig. 3. The UV variation of AG Dra during the three active phases observed with the IUE satellite. From top to bottom: the far–UV continuum at 1340 Å, the near–UV continuum at 2860 Å, N v λ1240, He II λ1640, and He II/F_{1340A}. All the fluxes are corrected for an interstellar extinction of E_{B-V}=0.06.

star's Zanstra temperature, did not change during the November 1980 rising phase, but largely decreased later on. We also note that the behaviour of the continuum and emission line flux during the "secondary" maximum and in the declining phases did not follow a common trend during the three active phases.

The high resolution IUE observations have disclosed the presence of a hot (N v), intermediate velocity (–200/300 km s^{-1}) wind which is present at least during the major outbursts (in 1981 and 1994). According to Viotti et al. (1983) this wind should arise from the hot WD, and we argue that it should originate from a lower gravity envelope of the WD during outburst.

Figure 4 shows the UV–to–optical energy distribution of AG Dra one month after the first light maximum, and in the following minimum phase. During outburst the flux increase has been very large in the far–UV, which is dominated by the tail of the hot star radiation. There is also an indication of a large Balmer jump. The flux increase during outburst was significant also at longer wavelengths. In particular we remark from the figure a 40% variation in the I–band, which implies that at maximum the "nebular" emission largely contributed also to the near–IR radiation of AG Dra. We cannot discard the possibility of a non–negligible contribution of the nebular continuum (f-f and f-b) to the longwave energy distribution also at minimum. In any case, both the VRI colours and the photospheric line depths might be affected by the nebular continuum, and they should therefore be used with some care in the determination of the stellar temperature and surface gravity.

AG Dra is surrounded by an extended nebula, ionized by the far–UV radiation of the hot dwarf, which is partly, or mostly formed from the K–star wind. The UV spectroscopy suggests that the CNO composition of the nebula is peculiar, with low C/N and (C+N)/O ratios (0.63 and 0.43, respectively), which is typical of metal poor cool giant atmospheres after CN cycle burning and a first dredge up phase (maybe plus mass transfer effects) (Schmid & Nussbaumer 1993). In this regard, it would be interesting to determine the chemical composition of the cool star atmosphere which was not yet done so far.

In quiescence, during the orbital motion the ionized nebula is partially occulted by the red star which explains the very broad minimum in U. EXOSAT observations at phase 0.50 gave no indication of an eclipse, which could be due either to the orbit inclination smaller than 90°, or to a very short duration of the eclipse combined with a slight phase shift. During the active phases, the increased flux of far–UV photons ionizes a much more extended region, which is masking the occultation effects. The major active phases seem to begin at the same orbital phase (0.1–0.2) which might suggest a link between orbital motion and outburst. This and the nearly regular recurrence time of the major outbursts could be understood if the orbit is eccentric, but the radial velocity curve gives no indication of a measurable orbital eccentricity (Kenyon & Garcia 1986, Mikolajewska et al. 1995). Alternatively, if the cool star is filling, or nearly filling its Roche lobe, an even small eccentricity or an increase of the surface activity of the red star, would substantially increase the accretion rate producing the outburst.

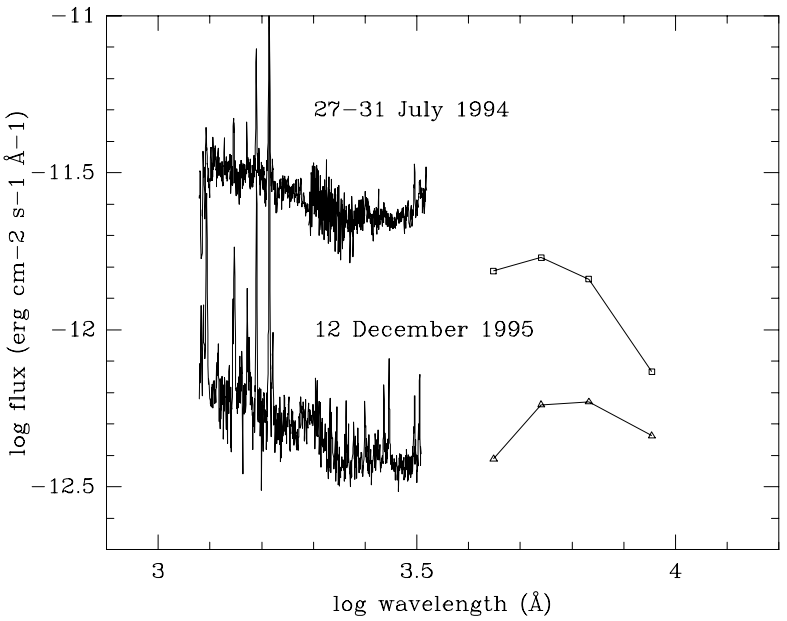

Fig. 4. Ultraviolet (IUE)–optical (BVRI) energy distribution of AG Dra during the 1994 outburst (27-31 July 1994), and at minimum (11 December 1995).

Acknowledgements: This work is based on data obtained from the IUE Data Bank, and on observations by IUE collected at the IUE Observatory of ESA at VILSPA within approved IUE programmes, or as targets–of–opportunity. We are grateful to the many amateurs who have continuously monitored AG Dra during the different phases of activity, and whose data are providing a precious database for this and future investigations. R.V. was partially supported by funds of the Agenzia Spaziale Italiana (ASI) under contract ASI 94-RS-59. JG is supported by the Deutsche Agentur für Raumfahrtangelegenheiten (DARA) GmbH under contract FKZ 50 OR 9201.

References

Anderson C.M., Cassinelli J.P., Sanders W.T., 1981, ApJ 247, L127
Bickert K., Greiner J., Stencel R.E., 1996, this volume p. 225
Greiner J., Bickert K., Luthardt R., Viotti R., Altamore A., Gonzalez-Riestra G., 1996, this volume p. 267
Huang C.-C., Friedjung M., Zhou Z.X., 1994, A&AS 106, 413
Iijima T., Vittone A., Chochol D., 1987, A&A 178, 203
Kafatos M., Meyer S.R., Martin I., 1993, ApJS 84, 201
Kenyon S.J., Garcia M.R., 1986, AJ 91, 125
Lutz J.H., Lutz T.E., Dull J.D., Kolb D.D., 1987, AJ 94, 463

Meinunger L., 1979, IBVS No. 1611
Mikolajewska J., Kenyon S.J., Mikolajewski M., et al., 1995, AJ 109, 1289
Mürset U., Nussbaumer H., Schmid H.M., Vogel M., 1991, A&A 248, 458
Piro L., Cassatella A., Spinoglio L., Viotti R., Altamore A., 1985, IAU Circ. 4082
Robinson L., 1969, Peren. Sviosdi 16, 587
Schmid H.M., Nussbaumer H., 1993, A&A 268, 159
Viotti R., Ricciardi O., Ponz D., et al., 1983, A&A 119, 285
Viotti R., Altamore A., Baratta G.B., et al., 1984, ApJ 283, 226
Viotti R., Giommi P., Friedjung M., Altamore A., 1995, Proc. Abano-Padova Conference on Cataclysmic Variables, A. Bianchini et al. (eds.), ASSL 205, 195

UV and X-Ray Monitoring of AG Draconis During the 1994/1995 Outbursts*

J. Greiner[1], K. Bickert[1], R. Luthardt[2], R. Viotti[3], A. Altamore[4], R. González-Riestra[5]**

[1] Max-Planck-Institut für Extraterrestrische Physik, 85740 Garching, Germany
[2] Sternwarte Sonneberg, 96515 Sonneberg, Germany
[3] Istituto di Astrofisica Spaziale, CNR, Via Enrico Fermi 21, 00044 Frascati, Italy
[4] Dipartimento di Fisica E. Amaldi, Università Roma III, 00146 Roma, Italy
[5] IUE Observatory, ESA, Villafranca del Castillo, 28080 Madrid, Spain

Abstract. The recent 1994-1995 active phase of AG Draconis has given us for the first time the opportunity to follow the full X-ray behaviour of a symbiotic star during two successive outbursts and to compare with its quiescence X-ray emission. With *ROSAT* observations we have discovered a remarkable decrease of the X-ray flux during both optical maxima, followed by a gradual recovering to the pre-outburst flux. In the UV the events were characterized by a large increase of the emission line and continuum fluxes, comparable to the behaviour of AG Dra during the 1980-81 active phase. The anticorrelation of X-ray/UV flux and optical brightness evolution is shown to very likely be due to a temperature decrease of the hot component. Such a temperature decrease could be produced by an increased mass transfer to the burning compact object, causing it to slowly expand to about twice its original size.

1 Introduction

The symbiotic star AG Draconis (BD +67°922) plays an outstanding role inside the group of symbiotic stars (binary systems consisting of a cool, luminous visual primary and a hot compact object (white dwarf, subdwarf) as secondary component) because of its high galactic latitude (b^{II}=+41°), its large radial velocity of v_r=−148 km/s and its relatively early spectral type (K). AG Dra is probably a metal poor symbiotic binary in the galactic halo.

The historical light curve of AG Dra is characterized by a sequence of active and quiescent phases (e.g. Robinson 1969) The activity is represented by 1–2 mag light maxima (currently called *outbursts* or *eruptions*) frequently followed by one or more secondary maxima. Between the active phases AG Dra is spending long periods (few years to decades) at minimum light with small (0.1 mag) semiregular photometric variations in B and V with pseudo-periods of 300-400 days (Luthardt 1990). However, in the U band regular variations with amplitudes of 1 mag and a period of 554 days have been discovered by Meinunger (1979).

*Based on observations made with the *International Ultraviolet Explorer* collected at the Villafranca Satellite Tracking Station of the European Space Agency, Spain.
**Also Astronomy Division, Space Science Department, ESTEC.

This periodicity is associated with the orbital motion of the system, as confirmed by the radial velocity observations of Kenyon and Garcia (1986).

The optical spectrum of AG Dra is typical of a symbiotic star, with a probably stable cool component which dominates the yellow-red region, and a largely variable "nebular" component with a strong blue-ultraviolet continuum and a rich emission line spectrum (e.g. Boyarchuk 1966). According to most authors the cool component is a K3 giant, which together with its large radial velocity and high galactic latitude, would place AG Dra in the halo population at a distance of about 1.2 kpc, 0.8 kpc above the galactic plane. More recently, Huang et al. (1994) suggested that the cool component may be of spectral type K0Ib, which would place it at a distance of about 10 kpc, at z = 6.6 kpc.

The UV continuum and line flux is largely variable with the star's activity. Viotti et al. (1984) studied the IUE spectra of AG Dra during the major 1980–1983 active phase, and found that the outburst was most energetic in the ultraviolet with an overall rise of about a factor 10 in the continuum, much larger than in the visual, and of a factor 2–5 in the emission line flux.

First X-ray observations of AG Dra during the quiescent phase with *Einstein* before the 1981-1985 series of eruptions revealed a soft spectrum (Anderson et al. 1981). The data are consistent with a blackbody source of kT=0.016 keV (Kenyon 1988) in addition to the bremsstrahlung source (kT=0.1 keV) suggested by Anderson et al. (1981). *EXOSAT* was pointed on AG Dra four times during the 1985–86 minor active phase, which was characterized by two light maxima in February 1985 and January 1986. These observations revealed a large X-ray fading with respect to quiescence (Piro 1986), the source being at least 5–6 times weaker in the EXOSAT thin Lexan filter in March 1985, and not detected in February 1986 (Viotti et al. 1995).

In June/July 1994 AG Dra went into a major outburst (Graslo et al. 1994), after which it gradually declined to the quiescent level in November 1994. Like the 1981–82 and 1985–86 episodes, AG Dra underwent a secondary outburst in July 1995. Here, we use all available *ROSAT* data to document the X-ray light curve of AG Dra over the past 5 years and report on the results of the coordinated *ROSAT* /*IUE* campaign during the 1994/1995 outbursts.

2 IUE Observations

AG Dra was observed by IUE as a Target of Opportunity starting on June 29, 1994. Observations have continued until February 1996, covering therefore the 1994 and 1995 outbursts as well as the period between them and the return to quiescence. In general, priority was given to low resolution spectra, but high resolution data were also obtained on most of the dates. For most of the low resolution images, both IUE apertures were used in order to have in the Large Aperture the continuum and the emission lines well exposed and in the Small Aperture (not photometric) the strongest emission lines (essentially HeII 1640 Å) not saturated. The fluxes from the Small Aperture spectra were corrected for

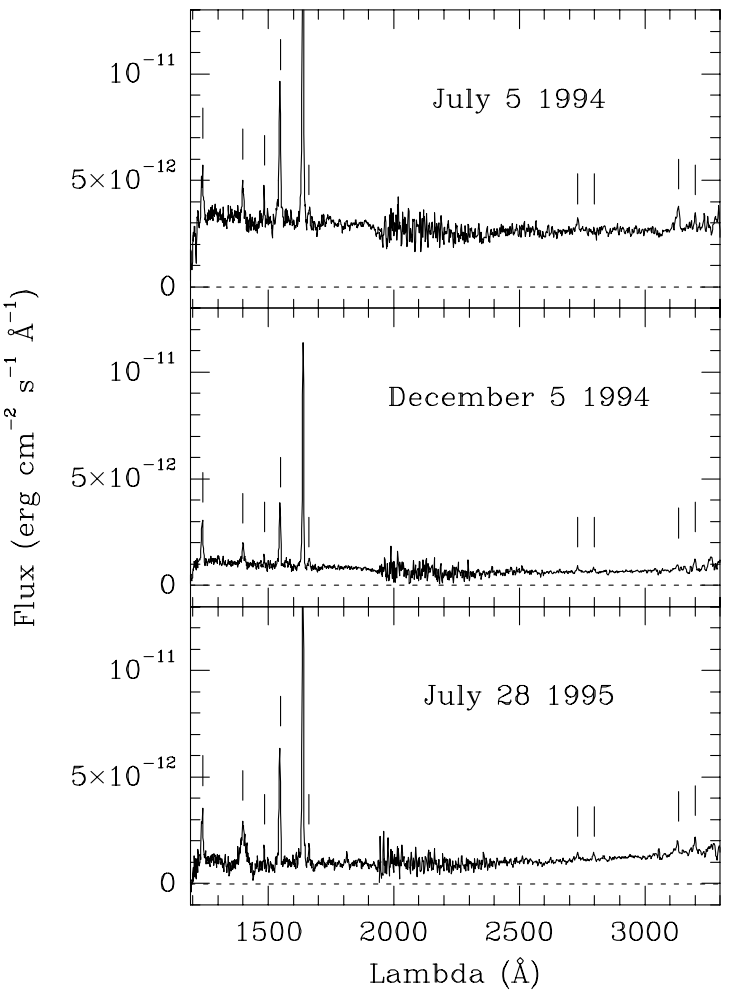

Fig. 1. IUE spectra of AG Dra at three different dates during the 1994-1995 activity phase: during the 1994 outburst (top), during the "quiescent" state between the outbursts (middle) and during the second outburst (bottom). The strongest line in the three spectra is HeII 1640 Å. The lines marked in the spectra are: NV 1240 Å, the blend SiIV + OIV] 1400 Å, NIV] 1486 Å, CIV 1550 Å, OIII] 1663 Å, HeII 2733 Å, MgII 2800 Å, OIII 3133 Å and HeII 3202 Å.

the smaller aperture transmission by comparison with the non-saturated parts of the Large Aperture data. Some representative IUE spectra are shown in Fig. 1.

The behaviour of the continuum and line intensities is shown in Fig. 2. All the fluxes are corrected for an interstellar absorption of E(B-V)=0.06 (Viotti et al. 1983). The feature at 1400 Å is a blend, unresolved at low resolution of the Si IV doublet at 1393.73 and 1402.73 Å, the OIV] multiplet (1399.77, 1401.16, 1404.81

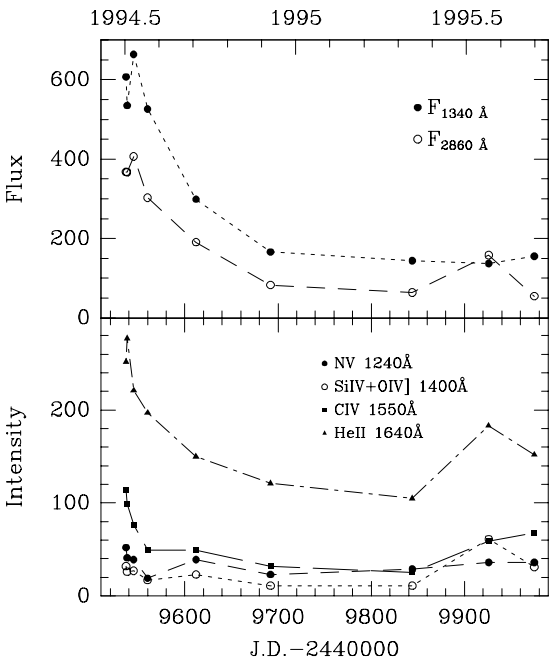

Fig. 2. Evolution of the UV continuum and emission lines of AG Dra during the 1994-1995 outburst. Units of continuum fluxes are 10^{-14} erg cm^{-2} s^{-1} Å^{-1}, and of line intensities 10^{-12} erg cm^{-2} s^{-1}. All the measurements are corrected for an interstellar reddening of E(B-V)=0.06.

and 1407.39 Å), and S IV] 1402.73 Å. O IV]1401.16 is the dominant contributor to the blend. Because of the variable intensity of the lines, at low resolution the 1400 Å feature shows extended wings with variable extension and strength (Fig. 1). The two continuum regions were chosen, as in previous works, for being less affected by the emission lines, and for being the 1340 Å respresentative of the continuum of the hot source (nearly the Rayleigh-Jeans tail of a 10^5 K blackbody), and the 2860 Å region representative of the HII Balmer continuum emission (see for instance Fernández-Castro et al. 1995).

3 ROSAT Observations

3.1 Observational Details

All-Sky-Survey AG Dra was scanned during the All-Sky-Survey over a time span of 10 days. The total observation time resulting from 95 individual scans adds up to 2.0 ksec.

Pointed Observations Several dedicated pointings on AG Dra have been performed in 1992 and 1993 with the ROSAT PSPC. All pointings were performed with the target on-axis. During the last *ROSAT* observation of AG Dra with the PSPC in the focal plane (already as a TOO) the Boron filter was erroneously left in front of the PSPC after a scheduled calibration observation.

When AG Dra was reported to go into outburst (Granslo et al. 1994) we immediately proposed for a target of opportunity observation (TOO) with ROSAT. AG Dra was scheduled to be observed during the last week of regular PSPC observations on July 7, 1994, but due to star tracker problems no photons were collected. For all the later *ROSAT* observations only the HRI could be used after the PSPC gas has been almost completely exhausted. Consequently, no spectral information is available for these observations. The first HRI observation took place on August 28, 1994, about 4 weeks after the optical maximum.

3.2 The X-Ray Lightcurve of AG Dra

The mean ROSAT PSPC countrate of AG Dra during the all-sky survey was determined to (0.99±0.15) cts/sec. Similar countrates were detected in several PSPC pointings during the quiescent time interval 1991–1993. The X-ray light curve (mean countrate over each pointing) of AG Dra as deduced from the All-Sky-Survey data taken in 1990, and 11 *ROSAT* PSPC pointings as well as 7 HRI pointings taken between 1991 and 1996 is shown in Fig. 3. The countrates of the HRI pointings have been converted with a factor of 7.5 and are also included in Fig. 3. This 5 yrs X-ray light curve displays several features:

1. The X-ray intensity has been more or less constant between 1990 and the last observation (May 1993) before the optical outburst. Using the mean best fit blackbody model with kT = 15 eV and the galactic column density $N_H = 3.15 \times 10^{20}$ cm^{-2} (see below), the unabsorbed intensity in the ROSAT band (0.1–2.4 keV) is 2.5×10^{-9} erg cm^{-2} s^{-1}.
2. During the times of the optical outbursts the observed X-ray flux drops substantially. The observed maximum amplitude of the intensity decrease is nearly a factor of 100. Due to the poor sampling we can not determine whether the amplitudes of the two observed X-ray intensity drops are similar. With the lowest intensity measurement being an upper limit, the true amplitude is certainly even larger.
3. Between the two X-ray minima the X-ray intensity nearly reached the pre-outburst level, i.e. the relaxation of whatever parameter caused these drops was nearly complete. We should, however, note that the relaxation to the pre-outburst level was faster at optical wavelength than at X-rays, and also was faster in the B band than in the U band. In December 1994 the optical V brightness ($\approx 9\overset{\mathrm{m}}{.}5$) was nearly back to the pre-outburst magnitude, while the X-ray intensity was still a factor of 2 lower than before the outburst.
4. The quiescent X-ray light curve shows two small, but significant intensity dips in May 1992 and April/May 1993. The latter and deeper dip coincides with the orbital minimum in the U lightcurve (Meinunger 1979, Skopal 1994).

3.3 The X-Ray Spectrum of AG Dra in Quiescence

For spectral fitting of the all-sky-survey data the photons in the amplitude channels 11–240 (though there are almost no photons above channel 50) were binned

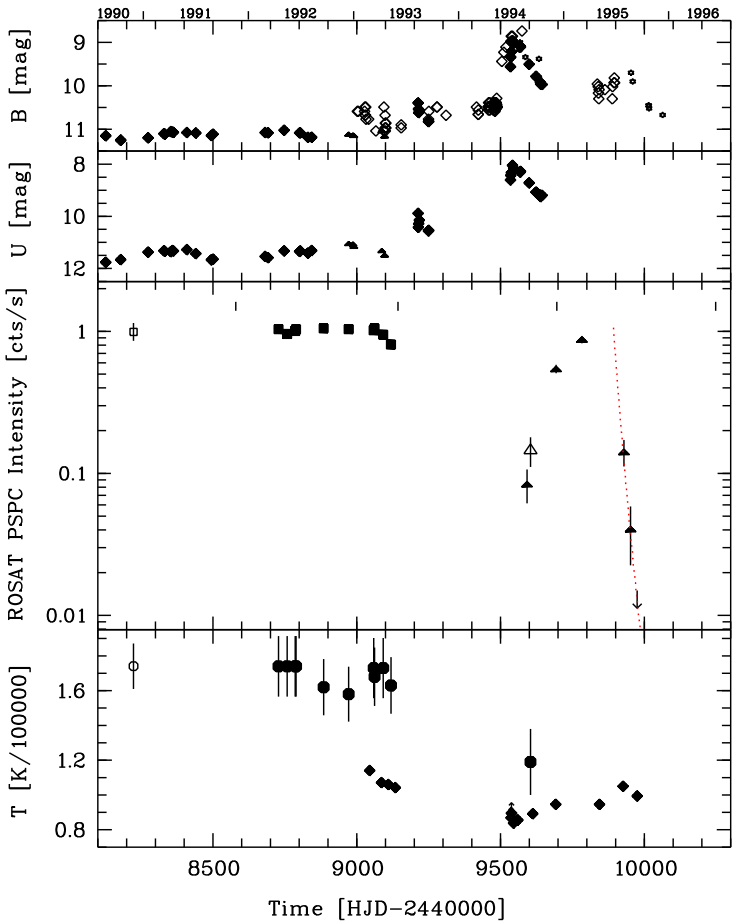

Fig. 3. The X-ray and optical light curve of AG Dra over the past 5 years. The two top panels show the U and B band variations as observed at Sonneberg Observatory (filled losanges = photoelectric photometry, open losanges = photographic sky patrol), Skalnate Pleso Observatory (Hric et al. 1994; filled triangles), and italian amateurs (Montagni et al. 1996; stars). The large middle panel shows the X-ray intensity as measured with the *ROSAT* satellite: filled squares denote PSPC observations, filled triangles are HRI observations with the countrate transformed to PSPC rates (see text), and the open triangle is the Boron filter observation corrected for the filter transmission. Statistical errors (1σ) are overplotted; those of the PSPC pointings are smaller than the symbol size. The vertical bars at the top indicate the minima of the U band lightcurve (Skopal 1994). The dotted line shows the fit of an expanding and cooling envelope to the X-ray decay light curve. The lower panel shows temperature estimates from blackbody fits to the *ROSAT* X-ray data (filled circles) and from the HeII(λ1640) flux to continuum flux at λ1340 Å as determined from the IUE spectra and assuming E(B–V)=0.06 (=Zanstra temperatures, filled losanges).

with a constant signal/noise ratio of 9σ. The fit of a blackbody model with all parameters free results in an effective temperature of $kT_{bb} = 11$ eV.

We investigated the possibility of X-ray spectral changes with time. First, we kept the absorbing column fixed at its galactic value and determined the temperature being the only fit parameter. We find no systematic trend of a temperature decrease (lower panel of Fig. 3). Second, we kept the temperature fixed (at 15 eV in the first run and at the best fit value of the two parameter fit in the second run) and checked for changes in N_H, again finding no correlation. Thus, no variations of the X-ray spectrum could be found along the orbit.

The independent estimate of the absorbing column towards AG Dra from the X-ray spectral fitting indicates that the detected AG Dra emission experiences the full galactic absorption. While fits with N_H as free parameter systematically give values slightly higher than the galactic value (which might lead to speculations of intrinsic absorption), we assess the difference to be not significant due to the strong interrelation of the fit parameters given the energy resolution of the PSPC and the softness of the X-ray spectrum. We will therefore use the galactic N_H value (3.15×10^{20} cm^{-2} according to Dickey and Lockman 1990) in the following discussion.

With fixed N_H the mean temperature during quiescence is about 14–15 eV, corresponding to 160000–175000 K. These best fit temperatures are plotted in a separate panel below the X-ray intensity (Fig. 3). The variations in temperature during the quiescent phase are consistent with a constant temperature of the hot component of AG Dra.

3.4 The X-Ray Spectrum of AG Dra in Outburst

As noted already earlier (e.g. Friedjung 1988), the observed fading of the X-ray emission during the optical outbursts of AG Dra can be caused by either a temperature decrease of the hot component or an increased absorbing layer between the X-ray source and the observer. In order to evaluate the effect of these possibilities, we have performed model calculations using the response of the *ROSAT* HRI. In a first step, we assume a 15 eV blackbody model and determine the increase of the absorbing column density necessary to reduce the *ROSAT* HRI countrate by a factor of hundred. The result is a factor of three increase. In a second step we start from the two parameter best fit and determine the temperature decrease which is necessary to reduce the *ROSAT* HRI countrate at a constant absorbing column (3.15×10^{20} cm^{-2}). We find that the temperature of the hot component has to decrease from 15 to 10 eV, or correspondingly from 175000 K to 115000 K.

The only ROSAT PSPC observation (i.e. with spectral resolution) during the optical outburst is the one with Boron filter. The three parameter fit as well as the two parameter fit give a consistently lower temperature. But since the Boron filter cuts away the high-end of the Wien tail of the blackbody, and we have only 19 photons to apply our model to, we do not regard this single measurement as evidence for a temperature decrease during the optical outburst.

What seems to be excluded, however, is any enhanced absorbing column during the Boron filter observation. The best fit absorbing column of the three parameter fit is 4.4×10^{20} cm^{-2}, consistent with the best fit absorbing column during quiescence. Since the low energy part of the spectrum in the PSPC is not affected by the Boron filter except a general reduction in efficiency by roughly a factor of 5, any increase of the absorbing column would still be easily detectable. For instance, an increase of the absorbing column by a factor of two (to 6.3×10^{20} cm^{-2}) would absorb all photons below 0.2 keV and would drop the countrate by a factor of 50 contrary to what is observed.

4 Discussion

4.1 Quiescent UV Emission

UV observations show that the hot components of symbiotic stars are located in the same quarters of the Hertzsprung-Russell diagram as the central stars of planetary nebula (Mürset et al. 1991). Due to the large binary separation in symbiotic systems the present hot component (or evolved component) should have evolved nearly undisturbed through the red giant phase. However, presently the outermost layers of the white dwarf might be enriched in hydrogen rich material accreted from the cool companion.

The far-UV radiation of the WD is ionizing a circumstellar nebula, mostly formed (or filled in) by the cool star wind. The UV spectrum in quiescence is the usual in symbiotic systems: a continuum increasing toward the shortest wavelengths with strong narrow emission lines superimposed. The most prominent lines in the quiescence UV spectrum of AG Dra are, in order of decreasing intensity: HeII 1640 Å, CIV 1550 Å, NV 1240 Å, the blend of SiV and OIV] at 1400 Å, NIV] 1486 Å and OIII] 1663 Å. The continuum becomes flatter longward approximately 2600 Å due to the contribution of the recombination continuum originated in the nebula. Although both continuum and emission lines have been found to be variable during quiescence (e.g. Mikolajewska et al. 1995), there is no clear relation with the orbital period of the system. The ratio intensity of the recombination He II 1640Å line to the far-UV continuum at 1340 Å suggests a Zanstra temperature of around 1.0-1.1$\times10^5$ K during quiescence (see Fig. 3).

4.2 Quiescent X-Ray Emission

The X-Ray spectrum Previous analyses of X-ray emission of symbiotic stars have been interpreted either with blackbody emission from the hot component (Kenyon and Webbink 1984, Jordan et al. 1994) or with bremsstrahlung emission from a hot, gaseous nebula (Kwok and Leahy 1984). Our ROSAT PSPC spectra of AG Dra show no hint for any hard X-ray emission. The soft spectrum is well fitted with a blackbody model. A thermal bremsstrahlung fit is not acceptable to this soft energy distribution. There is also no need for a second component as proposed by Anderson et al. (1981).

With an adopted distance of 1 kpc and using the blackbody fit parameters while N_H was fixed at its galactic value, the unabsorbed bolometric luminosity of the hot star during quiescence (1990–1993) is 1.4×10^{36} (D/1 kpc)^2 erg/s (or equivalently 370 (D/1 kpc)^2 $L_\odot$) with an uncertainty of a factor of a few due to the errors in the absorbing column and the temperature. The blackbody radius is derived to be $R_{bb} = 1.33\times10^9$ cm (D/1 kpc).

Wind Mass Loss and Accretion Accepting the high luminosity during quiescence and consequently assuming that the hot component in the AG Dra system is in (or near to) the hydrogen burning regime, the companion has to supply the matter at the high rate of consumption by the hot component. The spectral classification of the companion in the AG Dra binary system, in particular its luminosity class, is very uncertain. The commonly used K3III classification would imply a mass loss rate of $(0.2\text{–}7)\times10^{-10}$ $M_\odot$/yr according to the formula of Reimers (1975) or that of De Jager et al. (1988) for population I objects. In contrast, a K0 supergiant could have a mass loss rate of about 5×10^{-8} $M_\odot$/yr, more appropriate for the burning state of the compact object in AG Dra.

While a K3III giant of 1.1 $M_\odot$ would not fill its Roche lobe, a K0Ib supergiant would by far overfill its Roche lobe for any WD mass. Thus, in the case of a K3III companion the mass transfer to the WD would have to occur via Bondi-Hoyle accretion from the wind of the giant which by itself is already too low by orders of magnitude to sustain a burning compact object. Alternatively, a supergiant could either supply a high mass loss for wind accretion or could even feed an accretion disk around the WD by Roche lobe overflow.

We therefore think that in order to sustain the high mass comsumption of the compact object in AG Dra, the companion must be at least a bright giant to fill its Roche lobe. Adopting a bright giant solution, the distance to AG Dra would be of the order of 4 kpc, and thus the luminosity would be 2.2×10^{37} erg/s. The implied compact object mass would be 0.4 $M_\odot$ (assuming the core mass-luminosity relation $L/L_\odot \approx 4.6\times10^4$ ($M_{core}/M_\odot - 0.26$) according to Iben and Tutukov 1989), and the mass ratio 13.

4.3 X-Ray Emission During the Outbursts

Using our finding of an anticorrelation of the optical and X-ray intensity and the lack of considerable changes in the temperature of the hot component during the 1994/95 outburst of AG Dra, we propose the following rough scenario. (1) The white dwarf is already burning hydrogen stably before the outburst. (2) Increased mass transfer, possibly episodic, from the cool companion results in a slow expansion of the white dwarf. (3) The expansion is restricted either due to the finite excess mass accreted or by the wind driven mass loss from the expanding photosphere. This wind possibly also suppresses further accretion onto the white dwarf. The photosphere is expected to get cooler with increasing radius. (4) The white dwarf is contracting back to its original state once the accretion rate drops below the burning rate. Since the white dwarf is very sensitive it is not expected to return into a steady state immediately (Paczynski and Rudak 1980).

Instead, it might oscillate around the equilibrium state giving rise to secondary or even a sequence of smaller outbursts following the first one.

The scenario of an expanding white dwarf photosphere due to the increase in mass of the hydrogen-rich envelope has already been proposed by Sugimoto et al. (1979). The expansion velocity was shown to be rather low (Fujimoto 1982). If we assume that the luminosity remains constant during this expansion, and for the moment also assume that the change in the envelope mass is small during the early phase (justified by the result; see below) then we can determine the expansion velocity (or equivalently the excess accretion rate $\dot{M} - \dot{M}_{\rm RG}$) simply by folding the corresponding temperature decrease by the response of the ROSAT detector. Fitting the countrate decrease of a factor of 3.5 within 23 days (from 0.14 cts/s on HJD 9929 to 0.04 cts/s on HJD 9952) we find that

$$\left(\frac{\dot{M} - \dot{M}_{\rm RG}}{10^{-6} M_{\odot} yr^{-1}} \right) \approx 0.27$$

i.e. the necessary change in the accretion rate is as small as only 27%. This translates into an expansion rate of ≈2 m/s. The corresponding modelled countrate decrease is shown as the dotted line in Fig. 3, and the extrapolation to the quiescent countrate level gives an expected onset of the expansion at JD ≈ 9891.

Since we did not observe the X-ray intensity decline during the first outburst, and have no appropriate data yet for the X-ray intensity rise after the second outburst, the following estimates are only crude. Assuming similar durations of the first and the second outburst, we find that during each event the radius of the white dwarf roughly doubles (from 0.02 $R_{\odot}$ to 0.043 $R_{\odot}$) while the temperature decreases by about 35% (from 14.8 eV to 9.5 eV for the two parameter fit).

4.4 Relation to the Class of Supersoft X-Ray Sources

With its soft X-ray properties AG Dra is very similar to the supersoft X-ray sources (SSS) which are characterized by very soft X-ray radiation (kT≈ 25–40 eV) of high luminosity (Greiner et al. 1991, Heise et al. 1994). Among the optically identified objects there are several different types of objects: close binaries like the prototype CAL 83 (Long et al. 1981), novae, planetary nebulae, and symbiotic systems. In addition to AG Dra, two other luminous symbiotic systems are known (RR Tel, SMC 3) which both are symbiotic novae.

The similarity in the quiescent X-ray properties of AG Dra to those of the symbiotic novae RR Tel and SMC 3 might support the speculation that AG Dra is a symbiotic nova in the post-outburst stage for which the turn-on is not documented. We have checked some early atlasses such as the Bonner Durchmusterung, but always find AG Dra at the $10–11^{\rm m}$ intensity level. Thus, if AG Dra should be a symbiotic nova, its hypothetical turn on would have occurred before 1855. We note, however, that there are a number of observational differences between AG Dra and RR Tel which would be difficult to understand if AG Dra were a symbiotic nova.

If AG Dra is not a symbiotic nova, it would be the first wide binary supersoft source (as opposed to the classical close binaries) the existence of which has been predicted by Di Stefano et al. (1996). These systems are believed to have donor companions more massive than the accreting white dwarf which makes the mass transfer unstable on a thermal timescale. Recent calculations have shown that there is a maximum mass ratio of about 7, above which no system survives. The mass ratio of 13 for AG Dra which results from adopting a luminosity class II companion is far above this upper limit and thus suggests that more work has to be done to improve our understanding of the system parameters in AG Dra and/or that of the mass transfer in high mass ratio binary systems.

5 Summary

The major results and conclusions can be summarised as follows:

- The X-ray spectrum in quiescence is very soft, with a blackbody temperature of about 15 eV.
- The quiescent bolometric luminosity of 1.4×10^{36} $(D/1\ kpc)^2$ erg/s suggests stable hydrogen burning in quiescence.
- The monitoring at X-rays and UV wavelengths did not yield any hints for a predicted eclipse during the U light minima.
- In order to sustain the high luminosity the companion is required to fill its Roche lobe, and consequently is assumed to be of luminosity class II. With this assumption, the distance of AG Dra would be about 4 kpc, the X-ray luminosity would suggest a low-mass white dwarf, and the mass ratio would exceed 10.
- During the optical outburst in 1994 the UV continuum increased by a factor of 10, the UV line intensity by a factor of 2 and the X-ray intensity dropped by at least a factor of 100. There is no substantial time lag between the variations in the different energy bands.
- There is no hint for an increase of the absorbing column during one X-ray observation with spectral resolution performed during the decline of the optical outburst in 1994. Instead, a temperature decrease is consistent with the X-ray data and also supported by the *IUE* spectral results.
- Modelling the X-ray intensity drop by a slowly expanding white dwarf with concordant cooling, we find that the necessary excess accretion rate is only 27% of the quiescent one. Accordingly, the white dwarf expands to approximately its double size within the about three months rise of the optical outburst. The cooling is moderate: the temperature decreases by only $\sim$35%.
- AG Dra could either be a symbiotic nova with a turn on before 1855, or the first example of the wide binary supersoft source class.

Acknowledgement: We are grateful to J. Trümper and W. Wamsteker for granting the numerous target of opportunity observations with *ROSAT* and *IUE* . JG is supported by the Deutsche Agentur für Raumfahrtangelegenheiten (DARA)

GmbH under contract FKZ 50 OR 9201. RV is partially supported by the Italian Space Agency under contract ASI 94-RS-59. The *ROSAT* project is supported by the German Bundesministerium für Bildung, Wissenschaft, Forschung und Technologie (BMBW/DARA) and the Max-Planck-Society.

References

Anderson C.M., Cassinelli J.P., Sanders W.T., 1981, ApJ 247, L127
Boyarchuk A.A., 1966, Astrofizika 2, 101
De Jager C., Nieuwenhuijzen H., van der Hucht K.A., 1988, A&A Suppl. 72, 259
Dickey J.M., Lockman F.J., 1990, Ann. Rev. Astron. Astrophys. 28, 215
Di Stefano R., et al. 1996, ApJ (in press)
Fernández-Castro T., González-Riestra R., Cassatella A., et al. 1995, ApJ 442, 366
Friedjung M., 1988, in "The symbiotic phenomenon", eds. J. Mikolajewska et al. , IAU Coll. 103, ASSL 145, p. 199
Fujimoto M.Y., 1982, ApJ 257, 767
Granslo B.H., Poyner G., Takenaka Y., Schmeer P., 1994, IAU Circ. 6009
Greiner J., Hasinger G., Kahabka P. 1991, A&A 246, L17
Heise J., van Teeseling A., Kahabka P., 1994, A&A 288, L45
Hric L., Skopal A., Chochol D., et al. 1994, Contrib. Astron. Obs. Skalnaté Pleso 24, 31
Huang C.C., Friedjung M., Zhou Z.X., 1994, A&AS 106, 413
Iben I., Tutukov A.V., 1989, ApJ 342, 430
Jordan S., Mürset U., Werner K., 1994, A&A 283, 475
Kenyon S.J., 1988, in "The symbiotic phenomenon", eds. J. Mikolajewska et al. , IAU Coll. 103, ASSL 145, p. 11
Kenyon S.J., Webbink R.F., 1984, ApJ 279, 252
Kenyon S.J., Garcia M.R., 1986, AJ 91, 125
Kwok S., Leahy D.A., 1984, ApJ 283, 675
Luthardt R., 1990, Contr. of the Astr. Obs. Skalnate Pleso, CSFR, Vol. 20, p. 129
Meinunger L., 1979, IVBS No. 1611
Mikolajewska J., Kenyon S.J., Mikolajewski M., et al. 1995, AJ 109, 1289
Montagni F., Maesano M., Altamore A., Viotti R., 1996, IBVS (subm.)
Mürset U., Nussbaumer H., Schmid H.M., Vogel M., 1991, A&A 248, 458
Paczynski B., Rudak B., 1980, Acta Astron. 82, 349
Piro L., 1986 (priv. comm.)
Reimers D., 1975, Mem. Soc. R. Sci. Liege 8, 369
Robinson L.J., 1969, Peremennye Zvezdy 16, 507
Skopal A., 1994, IBVS No. 4096
Sugimoto D., Fujimoto M.Y., Nariai K., Nomoto K., 1979, in White dwarfs and degenerate variable stars, IAU Coll. 53, eds. H.M. van Horn et al., Rochester: p. 280
Viotti R., Ricciardi O., Ponz D., et al. 1983, A&A 119, 285
Viotti R., Altamore A., Baratta G.B., Cassatella A., Friedjung M., 1984, ApJ 283, 226
Viotti R., Giommi P., Friedjung M., Altamore A., 1995, Proc. Abano-Padova Conference on Cataclysmic Variables: eds. A. Bianchini et al. , ASSL 205, 195

A Candidate Isolated Old Neutron Star

R. Neuhäuser[1], F.M. Walter[2], S.J. Wolk[2]

[1] Max-Planck-Institut für extraterrestrische Physik, D-85740 Garching, Germany
[2] Earth and Space Science Dept., State University of New York, Stony Brook NY 11794-2100, USA

Abstract. We report on the serendipitous detection of a bright, very soft ROSAT X-ray source, RX J1856.5–3754, near the R CrA molecular cloud. Walter, Wolk, & Neuhäuser (1996) very recently have argued that this is a nearby isolated neutron star. As the source has also been detected with the *Einstein Observatory* slew survey, the mean X-ray count rate (3.6 cts/sec, as observed with ROSAT) remained steady over a 14 year interval. The X-ray spectrum is close to that of a blackbody with kT=57 eV. The absorption column places it foreground to the R CrA molecular cloud, i.e. at a distance of less than 120 pc. There is no optical counterpart to V≈23, meaning that the X-ray to optical flux ratio exceeds 7000. The emitting area is 480 km^2 at a distance of 100 pc. From pulsar birthrates and the inferred number of supernova required to account for the heavy element abundance in the Galaxy, it is likely that the Galaxy is populated with about 10^8-10^9 neutron stars, of which only a small fraction has been discovered, yet. It has been proposed that a few thousand old, isolated (i.e., those not in binary systems) neutron stars may be detectable in the ROSAT All-Sky Survey as hot thermal sources, either from a cooling surface or from accretion of interstellar material. However, this is only the second promising candidate.

1 Introduction

It has been proposed that the Galaxy is populated with about 10^8 to 10^9 neutron stars. This follows either from an extrapolation of pulsar birthrates (Narayan & Ostriker 1990), or from the inferred number of supernovae required to account for the heavy element abundance in our Galaxy (Arnett, Schramm, & Truran 1989), if one assumes that a significant fraction of the supernovae produce neutron stars. Only about 700 neutron stars are known as rotation powered pulsars and about 1000 as pulsars powered by accretion (Taylor et al. 1995), so that there must be a very large number of undetected neutron stars in the Galaxy.

It has been proposed that old isolated (i.e., those not in binary systems) neutron stars (IONS) may be detectable as hot thermal sources, either from a cooling surface or from accretion of interstellar material (Helfand, Chanan, & Novick 1980). The expected emission peaks in the EUV/soft X-rays, with black body temperatures less than $\sim 10^6\ K$. Treves & Colpi (1991) suggested that about 5000 isolated neutron stars, accreting out of the interstellar medium, could be detectable in the ROSAT All Sky Survey (RASS). Blaes & Madau (1993) revised the estimate, concluding that for reasonable distributions of spatial velocities, some 2000 isolated neutron stars, accreting isotropically out of the

interstellar medium, should be detectable in the RASS. This estimate has not been verified, and more recent estimates are significantly smaller (e.g., Madau & Blaes 1994, Blaes, Warren, & Madau 1995).

Despite the optimistic projection of thousands of nearby, detectable IONS, evidence for only two such object has been presented to date (Stocke et al. 1995, Walter, Wolk, & Neuhäuser 1996). The identification of the source presented by Stocke et al. (1995) is ambiguous; based on its ASCA X-ray spectrum, which shows a hard X-ray tail (J. Stocke, private communication), and proximity to the nucleus of the bright galaxy NGC 1313, it may well be an extragalactic massive accreting compact halo object. We report here about the soft X-ray source RX J1856.5–3754, which first appeared as very bright but unidentified source in the RASS, and was later observed in detail with deep ROSAT pointed observations. For details on the X-ray satellite ROSAT and its intruments, we refer to Trümper (1983).

2 The ROSAT Source RX J1856.5–3754

It has recently been claimed (Walter, Wolk, & Neuhäuser 1996) that the soft X-ray source RX J1856.5–3754 is an IONS; see also the discussion by Wang (1996) about this source. RX J1856.5–3754 is a bright source projected on the R CrA molecular cloud, a region of on-going low- and intermediate-mass star formation; the source's galactic latitude is $l_{II} = -17°$. The X-ray flux of RX J1856.5–3754 has been observed best with our 6.3 ksec deep ROSAT pointed observation with the Position Sensitive Proportional Counter (PSPC). In the PSPC energy range (from 0.11 to 2.4 keV) the flux is $f_{\rm X} = (1.46 \pm 0.02) \cdot 10^{-11}\ erg\ cm^{-2} s^{-1}$.

The spectrum can be evaluated using the so-called X-ray hardness ratio, defined as follows. If $Z_{\rm s}$, $Z_{\rm h1}$, and $Z_{\rm h2}$ denote count rates for the ROSAT PSPC energy channels soft (0.1 to 0.4 keV), hard 1 (0.5 to 0.9 keV), and hard 2 (0.9 to 2.1 keV), respectively, we define hardness ratios HR 1 and HR 2 as follows:

$$\text{HR 1} = \frac{Z_{\rm h1} + Z_{\rm h2} - Z_{\rm s}}{Z_{\rm h1} + Z_{\rm h2} + Z_{\rm s}} \quad \text{and} \quad \text{HR 2} = \frac{Z_{\rm h2} - Z_{\rm h1}}{Z_{\rm h2} + Z_{\rm h1}} \tag{1}$$

The RASS hardness ratios of our source are as follows:

$$\text{HR 1} = -0.932 \pm 0.018 \quad \text{and} \quad \text{HR 2} = -0.679 \pm 0.071 \tag{2}$$

Hence, the spectrum is very soft. The X-ray spectrum as observed with our ROSAT PSPC pointed observation is shown in Walter et al. (1996).

We have performed spectral fits with several different models including two models on thermal plasma (Mewe and Raymond-Smith), see Tab. 1 for fit results. Additionally, it has to be noted that a power law fit gave $\alpha = 6.7 \pm 0.1$ and $n_{\rm H} = (4.0 \pm 0.1) \cdot 10^{20}\ cm^{-2}$ with $\chi^2_\nu = 4.9$ only. We conclude that the source spectrum can be fit best by a 57 eV black body, with an absorption column of $(1.4 \pm 0.1) \cdot 10^{20}\ cm^{-2}$ corresponding to $A_V = 0.1$ mag.

Table 1. X-ray spectral fits

model	$k \cdot T$ [eV]	$n_{\rm H}$ [10^{20} cm^{-2}]	χ^2_ν
blackbody	57 ± 1	1.4 ± 0.1	2.3
Mewe	68 ± 6	6.1 ± 0.1	2.5
Bremsstrahlung	1000 ± 100	2.1 ± 0.5	2.8
Raymond-Smith	54 ± 2	5.0 ± 0.2	3.8

The source is *not* a soft transient. It was first detected in the *Einstein Observatory* slew survey (1980) with ten photons correponding to 0.86 ± 0.42 counts per second. It is visible in the RASS (1990), and in our ROSAT PSPC (1992) and ROSAT High Resolution Image (HRI, 1994) pointed observations. There is no evidence for source variability on any timescale (from milliseconds to years).

It is possible to study variability of a time scale of hours in detail using the RASS data. The PSPC on-board ROSAT performed the All-Sky Survey scanning the sky in great circles. With a 2° diameter field of view each object is observed once in every $\sim$ 90 minutes for up to $\sim$ 30 *sec* per scan. Vignetting corrected RASS exposure times vary roughly with $1/\cos\beta$ where β denotes ecliptic latitude. The CrA area with our soft source has been observed during twelve scans, so that the patrol time is $\sim 12 \cdot 90$ minutes, i.e. two thirds of a day. In Fig. 1 , the RASS light curve is shown.

This supersoft X-ray source has not been studied in detail before, e.g. by groups searching particulary for IONS, because the hardness ratio HR 1 as observed in the RASS and as obtained from the Standard Analysis Software System (SASS) does not fulfil the formal criterion for "supersoft" sources (namely that HR 1 plus its error is smaller than -0.9), among which such IONS are expected (Greiner 1996). However, the source's HR 1 as observed in the RASS and as obtained from the Extended Scientific Analysis Software System (EXSAS) does fulfil this criterion, see above equ. 2. While SASS is used to evaluate all the RASS data, EXSAS is superior in some details and is used only for parts of the RASS data (that are requested by investigators). A possible reason for different results from SASS and EXSAS is that (among other different details in these software packages) SASS evaluates RASS data in strips (see above), while EXSAS can be run on merged strips, so that a more realistic background can be estimated.

3 The Nature of the Source

At the position of the source, the integrated column density through the R CrA molecular cloud is about $5 \cdot 10^{20}\ cm^{-2}$ (Wang 1994); this requires that the source be no more distant than the 130 *pc* distance to the cloud (Marraco & Rydgren 1981). Walter, Wolk, & Neuhäuser (1996) took a recent optical CCD image of

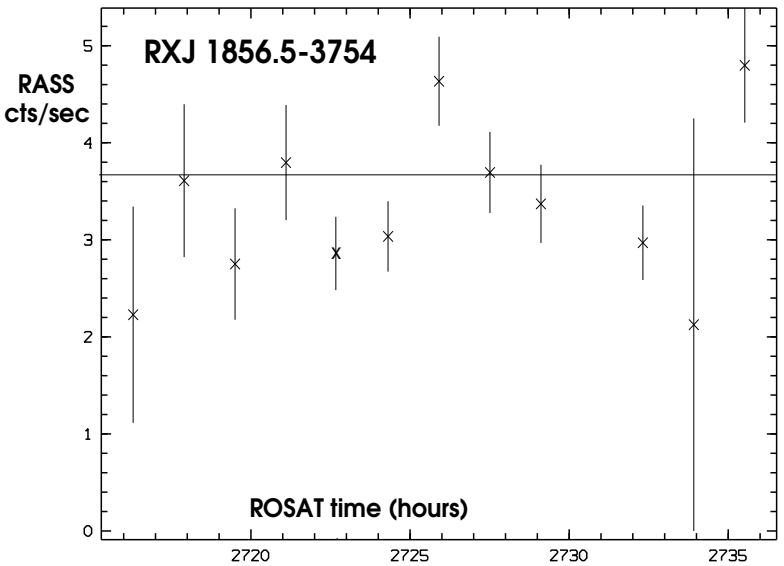

Fig. 1. RASS light curve of RX J1856.5–3754: RASS count rate in counts per second (corrected for vignetting and background) versus ROSAT observation time (in hours after the start of the ROSAT mission). The source has been observed in twelve consecutive RASS scans with exposure times between a few seconds and about 30 seconds. Error bars are one Gaussian sigma errors. No significant variability can be seen. The horizontal line indicates the mean RASS count rate of 3.67 ± 0.15 counts per second, consistent with the ROSAT PSPC pointed observation.

the area around the ROSAT HRI position. There is no optical counterpart down to $V = 23.1$ mag, yielding a lower limit to f_X/f_V of about 7000. The large f_X/f_V rules out *all* potential counterparts except isolated neutron stars. At a distance d the X-ray luminosity is $5 \cdot 10^{31}$ $(\frac{d}{100\ \mathrm{pc}})^2$ $erg\ s^{-1}$, and the emitting area is 480 $(\frac{d}{100\ \mathrm{pc}})^2$ km^2.

There is no known radio source or pulsar known at this position. Also, there is no ROSAT WFC, HEAO-1, EUVE, VLA, or IRAS source at or near this source (Walter, Wolk, & Neuhäuser 1996). The high X-ray to optical flux ratio f_X/f_V and the fact that the emission remains constant at time scales from milliseconds to 14 years rules out any accreting binary system or accretion powered system. The area suggests emission from the entire hot surface of a nearby IONS. The temperature is consistent with a cooling IONS with an age of $\sim 10^6$ years (Lattimer et al. 1994), or more, if the surfaces reheat due to internal friction (Reisennegger 1995). The luminosity and temperature are also consistent with the accretion heating model of Blaes & Madau (1993), for quasi-isotropic accretion by a neutron star moving at a velocity v of $\sim$ 50 $km\ s^{-1}$ (or little less) through a medium with a density of $n_H = 1\ cm^{-3}$. This object affords a unique opportunity to study the surface emission from a neutron star, unaffected by magnetospheric emission or by accretional processes in a binary system.

4 Future Observations

Our proposal (PI F.M. Walter) for observations of this IONS with the Hubble Space Telescope WFPC2 has been approved in order to obtain an optical identification (with expected $V = 27.4$ mag). Once we identify the counterpart, we will propose to obtain the spectral energy distribution in the optical and UV regime, the radius to within 25%, the parallax (to better than 20%), and the proper motion (if its transverse space velocity exceeds $\sim 10\ km/s$).

Another proposal (PI R. Neuhäuser) to obtain a broad band X-ray spectrum with the SAX LECS has been approved, too, in order to search for the 5 to 15 keV cyclotron resonance line emission expected from a strongly magnetized IONS and to determine the magnetic field from the line strength.

The study of IONS is useful for a number of fields in galactic astrophysics. Examination of non-pulsating IONS would permit study of the cooling of neutron star surfaces. If the IONS are heated by accretion from the interstellar medium, studies of the spatial structure of the interstellar medium on small spatial scales is possible. Since any detectable IONS must be nearby, it will be possible to study the kinematics of this population. Determination of the stellar radii would lead to improved constraints on the interior equation of state.

5 Summary

A very bright and soft, unidentified X-ray source has been observed with ROSAT. The X-ray spectrum can be fit best with a blackbody at kT = 57 eV. The absorbing column density is less than the one observed towards the R CrA molecular cloud, that appears to be in the background of this soft X-ray source. Hence, the X-ray source cannot be more distant than $\sim 130\ pc$. There is no variability on time scales from milliseconds to several years, so that any accretion powered system can be excluded as counterpart. No optical counterpart can be identified down to a limiting magnitude of $V = 23.1$ mag. Thus, together with the observed X-ray flux, we estimate the X-ray to optical flux ratio to be at least 7000, so that we can exclude any possible counterpart exept isolated old neutron stars.

Acknowledgement: We would like to thank J.T. Stocke, J.C.L. Wang, W. Becker, J. Greiner, and J. Trümper for useful conversation. Werner Becker also looked in detail into our ROSAT PSPC pointed observations and also could not find any significant variability on time scales down to milliseconds. The ROSAT project is supported by the German Bundesministerium für Bildung, Wissenschaft, Forschung und Technologie (BMBF/DARA) and the Max-Planck-Society.

References

Arnett W.D., Schramm D.N., Truran J.W., 1989, ApJL 339, L25
Blaes O., Madau P., 1993, ApJ 403, 690
Blaes O., Warren O., Madau P., 1995, ApJ 454, 370

Greiner J., 1996 (private comm.)
Helfand D.J., Chanan G.A., Novick R., 1980, Nat. 283, 337
Lattimer J.M., van Riper K.A., Prakash M., Prakash M., 1994, ApJ 425, 802
Madau P., Blaes O., 1994, ApJ 423, 748
Marraco H.G., Rydgren A.E., 1981, AJ 86, 62
Narayan R., Ostriker J.P., 1990, ApJ 352, 222
Reisenegger A., 1995, ApJ 422, 749
Stocke J.T., Wang Q.D., Perlman E.S., Donahue M.E., Schachter J., 1995, AJ 109, 1199
Taylor, et al., 1995, ApJS 88, 529
Treves A., Colpi M., 1991, A&A 241, 107
Trümper J., 1983, Adv. Space Res. 2, 241
Walter F.M., Wolk S.J., Neuhäuser R., 1996, Nat. 379, 233
Wang Q.D., 1994, in The Soft X-Ray Cosmos, E.M. Schlegel & R. Petre (eds.), AIP Conf. Proc. 313 (New York), 301
Wang Q.D., 1996, Nat. 379, 206

A Systematic Search for Supersoft X-Ray Sources in the ROSAT All-Sky Survey

J. Greiner

Max-Planck-Institut für Extraterrestrische Physik, 85740 Garching, Germany

Abstract. We have conducted a systematic search for supersoft X-ray sources using the ROSAT all-sky survey data. With the optical identification of the selected sources being almost complete, we discuss the statistics of the various source classes and their observability. Besides supersoft close binary sources this search also can be used to estimate the number of isolated neutron stars in the Galaxy, such as those described by Stocke et al. (1995) and Walter et al. (1996).

1 Introduction

Supersoft X-ray sources (SSS) are characterized by very soft X-ray radiation (most of the X-ray emission below 0.5 keV) of high luminosity. It is generally accepted that SSS involve steady nuclear burning on the surface of an accreting WD (van den Heuvel et al. 1992). ROSAT observations established SSS as a distinct class with somewhat more than 30 members known at present. While 16 sources belong to M 31, and a dozen to the Magellanic Clouds, only very few have been found in the Galaxy.

A simple scaling from the brightest supersoft X-ray sources in the Magellanic Clouds to galactic distances already shows that there are no such sources in our immediate neighbourhood. If CAL 83, the SSS prototype (Long et al. 1981), were at 1 kpc distance, we would expect a ROSAT PSPC countrate of 3000 cts/sec, much larger than the PSPC threshold intensity. Any such unabsorbed source in the solar neighbourhood would have forced the PSPC to switch off and it is safe to say that no such source has been detected in the ROSAT all-sky survey.

However, the intrinsic source luminosities are observed to vary from source to source by a factor of about 50, the mean temperatures of the WDs could be systematically lower in the Galaxy as compared to the Magellanic Clouds, and a moderate absorbing column could further dim the sources. We therefore have undertaken a systematic search of the ROSAT PSPC all-sky survey data for supersoft X-ray sources with emphasis on the galactic population.

2 Selection Criteria

We started with the list containing all detected X-ray sources of the all-sky survey in its version of March 1991 which contained about 100.000 sources (including detections of identical sources in overlapping strips). We applied a hardness ratio criterion $\mathrm{HR1} + \sigma_{\mathrm{HR1}} \leq -0.80$ which is fulfilled by 304 sources. The

hardness ratio HR1 is defined as the normalized count difference (N_{52-201} – N_{11-41})/(N_{11-41} + N_{52-201}), where N_{a-b} denotes the number of counts in the PSPC between channel a and channel b. After merging double and multiple detections from different strips at high ecliptic latitudes we are left with 165 sources. We have taken the results of each source from that strip in which the source has the largest distance to either edge of the strip. Finally, images in different energy bands were visually inspected to check for possible false detections, and to reduce spurious sources in bright supernova remnants (like Vela/Puppis). The final number of selected sources is 143.

This kind of hardness ratio selection has the implication of an implicit intensity selection. First, for decreasing brightness the error in the hardness ratio increases, and all sources with $\sigma_{HR1} \geq 0.2$ are exluded. Second, it also cuts away specific sources (like G or K stars) which are detected at high signal to noise ratio. This is due to the fact that these objects exhibit a faint hard component, and this is detected only for bright sources.

Finally we should note that the input list has been produced from source detections on the individual strips. At high ecliptic latitudes these strips overlap, and with the "survey II" processing which is done on adjacent sky fields instead of strips (and which will becaome available soon) a considerable improvement of the source detection and parameter estimation is possible.

3 Optical Identification and Source Statistics

A correlation with the Simbad database revealed probable source identifications for a total of 48 sources. Most of these identifications were single white dwarfs. Since we were not interested in discovering further WDs, and many of these WDs have been detected also in the extreme-ultraviolet sensitive Wide Field Camera (WFC), we have used the WFC source list to remove all sources from our master list which have been seen in the WFC (total number of 53). These sources were not considered for our own follow-up identification, but were left by purpose for the WFC consortium (and most of these were later identified as WDs).

The remaining sources have been observed optically by the author (mainly northern hemisphere) and the group of K. Beuermann (southern hemisphere). The majority of X-ray sources turned out to be magnetic cataclysmic variables, predominantly polars. The only galactic supersoft source (close binary) in this sample is RX J0019.8+2156 (Beuermann et al. 1995, Greiner & Wenzel 1995) while the other two are LMC/SMC sources (1E 0035.4–7230 and RX J0439.8–6809). Tab. 1 shows a breakdown of the sources on the individual source classes.

A few notes should be added to Tab. 1. The G and K star identifications (IDs) are probably systems with a WD in a close orbit, so after spectroscopic follow-up observations these two IDs will certainly be replaced. There is one additional object of presumably this type among the unidentified sources which also has a G star at the X-ray position. The only active galactic nuclei in our sample is the narrow-line Seyfert 1 (NLSy1) galaxy WPVS007, and many more are expected at somewhat harder hardness ratios (Greiner et al. 1996).

Table 1. The distribution among different classes of objects of supersoft X-ray sources which satisfy HR1 + $\sigma_{\rm HR1} \leq -0.80$. PN means planetary nebula, the other abbreviations are explained in the text.

Class type	Simbad correlation	newly identified	total
SSS	0	3	3
PN	2	0	2
PG1159 stars	0	1	1
symbiotics	2	1	3
single WDs	32	66	98
magnetic CVs	5	12	17
NLSy1	1	0	1
B stars	4	0	4
G stars	1	0	1
K stars	1	0	1
unidentified			12

4 Discussion

In total, only seven out of the more than 30 known supersoft sources are members of our sample, namely the above listed RX J0019.8+2108, 1E 0035.4–7230 and RX J0439.8–6809 plus the planetary nebula RX J0058.6–7146 (N 67) plus the three symbiotics RX J0048.4–7332 (SMC3), RR Tel and AG Dra. This demonstrates the "conservative" approach of our selection criterium. In fact, it is more effective for low-temperature sources like single white dwarfs or PG1159 stars. The above listed sources are the softest among the known population of SSS. As soon as a source has a temperature higher than about 40 eV and the PSPC detects a significant number of photons above channel 41 (0.4 keV) than the HR1 increases and shifts the source out of our hardness ratio window. That is, our sampling of supersoft sources is complete only for temperatures below about 30 eV.

The brightest of the non-identified sources has a PSPC countrate of 0.37 cts/s. Above this intensity the identification is complete. This implies that any galactic source radiating at the Eddington rate with a temperature in the 20–40 eV range would have been detected above a galactic latitude bII>12°. Relaxing the luminosity constraint by a factor of 10 increases the latitude limit only slightly to bII>15°.

A different approach in searching for supersoft sources is to look specifically for strongly absorbed sources in the galactic plane. Their energy distribution then is expected to be sharply peaked around 0.5–0.7 keV with higher energy photons missing due to the spectrum of the source, and lower energy photons absorbed. Such a source would have a relatively hard HR1 but a very soft HR2. Indeed, these criteria have led to the discovery of RX J0925.7–4758 (Motch

et al. 1994). From the results of the galactic plane survey identification these authors concluded that though sources radiating at the Eddington limit with a temperature below ~20 eV may be hidden in the galactic plane, sources at bII > 5–10° with temperatures above 40 eV and 4×10^{37} erg/s bolometric luminosity can be excluded. This supplements our finding for lower temperature sources.

Another possible class of soft X-ray sources are old, isolated neutron stars (IONS) accreting from the interstellar matter. Two sources have been proposed to be IONS, one of those (RX J1856.5–3754) is a bright source seen in the ROSAT all-sky survey (Walter et al. 1996). This source has been reported to have a best-fit blackbody temperature of below 60 eV. However, due to the distinct emission above 0.4 keV the hardness ratio is HR1=–0.29, far outside our selected range.

Such IONS are not expected to be easily visible in the optical range. All the unidentified sources of our sample have optical counterpart candidates brighter than 20th magnitude inside their corresponding error box. We therefore think that none of these sources might be another IONS candidate. This makes our search complete down to a limiting countrate of 0.1 cts/sec.

Since the temperature of the emitted radiation (assumed to be blackbody) is primarily determined by the ratio of accretion rate $\dot{M}$ to the fractional accreting area f (kT = 20 $(\dot{M}/\mathrm{f})^{1/4}$ eV with $\dot{M}$ in units of 10^{10} g/s, Blaes & Madau 1993), we can determine the range of accretion rates for which our search for supersoft sources is sensitive. Assuming isotropic accretion for simplicity, sources with accretion rates above 50×10^{10} g/s are too hot for our search (have a hardness ratio greater than −0.8), while below 0.05×10^{10} g/s the temperature and luminosity get too low to be detectable beyond 20 pc.

Acknowledgement: JG is extremely grateful to T. Fleming for the frequent information on the status of single WD identifications. JG is supported by the Deutsche Agentur für Raumfahrtangelegenheiten (DARA) GmbH under contract FKZ 50 OR 9201. The *ROSAT* project is supported by the German Bundesministerium für Bildung, Forschung, Wissenschaft und Technologie (BMBW/DARA) and the Max-Planck-Society. This research has made use of the Simbad database, operated at CDS, Strasbourg, France.

References

Beuermann K., Reinsch K., Barwig H., Burwitz V., de Martino D., Mantel K.-H., Pakull M.W., Robinson E.L., Schwope A.D., Thomas H.-C., Trümper J., van Teeseling A., Zhang E., 1995, A&A 294, L1

Blaes O., Madau P., 1993, ApJ 403, 690

Greiner J., Wenzel W., 1995, A&A 294, L5

Greiner J., Danner R., Bade N., Richter G.A., Kroll P., Komossa S., 1996, A&A (in press)

Long K.S., Helfand D.J., Grabelsky D.A., 1981, ApJ 248, 925

Motch C., Hasinger G., Pietsch W., 1994, A&A 284, 827

Stocke J.T., Wang Q.D., Perlman E.S., Donahue M., Schachter J.F., 1995, ANJ 109, 1199

van den Heuvel E.P.J., Bhattacharya D., Nomoto K., Rappaport S.A., 1992, A&A 262, 97

Walter F.M., Wolk S.J., Neuhäuser R., 1996, Nat. 379, 233

A Search for Optical Counterparts to Supersoft X-Ray Sources in the ROSAT Pointed Database

C.M. Becker, R. Remillard, S.A. Rappaport

Department of Physics, Massachusetts Institute of Technology, Cambridge, MA 02139

Abstract. We present a progress report of our program to identify optical counterparts of supersoft X-ray sources detected during pointed ROSAT PSPC observations. We generate a parent sample of ∼4100 supersoft sources by starting with the WGA (White et al. 1994) and ROSAT SRC (Zimmermann 1994) catalogs, extracting X-ray detections on the basis of softness (ROSAT HR1 ≤ -0.5), condensing multiple detections, and combining sources seen in both catalogs. This unwieldy sample is divided into four (occasionally overlapping) subclasses: (1) a flux limited sample (WGA only) encompassing ∼120 square degrees of sky, (2) an all-sky "extremely soft" sample (HR1 ≤ -0.8), (3) an optically bright all-sky sample with candidates $V \leq 14.5$, and (4) an all-sky sample near the nuclear burning white dwarf (NBWD) track in the HR1-HR2 plane, as defined with Monte Carlo simulations.
This program has been underway for about one year and has included seven observing runs at the MDM observatory at Kitt Peak, Arizona. In addition, numerous sources have been identified via catalog and literature searches. More observing runs are currently scheduled. Although no new NBWDs have been discovered yet, we have found many new supersoft AGN and emission stars, and a few new white dwarfs and CVs. By the conclusion of our program we will be able to set constraints on models concerning the population of NBWD, to understand the proportions of objects that make up the class of "supersoft X-ray sources", to investigate models for the supersoft nature of AGN, and (hopefully) to discover some new NBWD systems.

1 Introduction

One of the interesting contributions of the ROSAT satellite is the discovery of celestial objects possessing such soft X-ray spectra that over 75% of the counts are detected between 0.1 and 0.4 keV. These "supersoft X-ray sources" (SXS) themselves do not form a uniform group, but rather a collection of astrophysical systems including hot white dwarfs, stars with active coronae, cataclysmic variables (CVs), white dwarfs undergoing surface nuclear burning of accreted matter (NBWD), active galactic nuclei (AGN), and galaxies with warm halos.

A large number of SXS were discovered in the ROSAT All-Sky Survey (RASS) conducted during the first 6 months of the mission. The exposure time for a typical portion of the sky is ∼500 seconds but increases to be comparable to the pointed studies within 5° of the ecliptic poles. Between that time and November 1994, three years of pointed guest observations were accumulated with ROSAT. Two groups, one in Germany and one at NASA — Goddard Space Flight Center, independently searched these data for serendipitous sources, with each group

creating a catalog of their results. Each catalog contains about 50,000 detections, covers about ten percent of the sky, and yields a typical exposure time on any one source of about 11,000 seconds. Typical uncertainties in source location are $30''$ (90% confidence error radius). This database provides a new SXS sample that is complementary to the RASS and more comprehensive, in the overlapping energy bands, than the EUVE or ROSAT WFC surveys (400-500 sources each).

We have undertaken a large program to find optical counterparts to SXS detected in these new databases. Upon completing the optical search, follow-up studies, and additional supporting projects, we will be able to: (1) determine in a statistically meaningful manner the composition of the general class "supersoft X-ray source" (2) test theoretical predictions regarding mass transfer in NBWD systems by modeling the orbital structure, (3) test theoretical predictions regarding populations of NBWD in the Galaxy, (4) discover new NBWD systems to a flux ten times fainter than that of the only such unobscured galactic system, (5) determine whether preliminary conclusions drawn during similar studies of the RASS sample still hold at deeper flux limits, and (6) provide a sound model (incorporating X-ray data) as to the nature of supersoft AGN.

This paper is a report on our ongoing program. In Sect. 2 we discuss the selection of targets for optical observation, in Sect. 3 we provide the current status of the program, and in Sect. 4 we present preliminary results of our work.

2 Program Definition

The Goddard (WGA) and German (SRC) ROSAT catalogs report not only the position of each source, but also spectral information. We use the following spectral bands:

$$\begin{aligned} \mathrm{A} &= 11 \text{ - } 39 \text{ ADU} \approx 0.1 \text{ - } 0.4 \text{ keV} \\ \mathrm{B} &= 40 \text{ - } 85 \text{ ADU} \approx 0.4 \text{ - } 0.9 \text{ keV} \\ \mathrm{C} &= 86 \text{ - } 200 \text{ ADU} \approx 0.9 \text{ - } 2.0 \text{ keV}, \end{aligned}$$

and form two hardness ratios

$$\mathrm{HR1} = \frac{(\mathrm{C}+\mathrm{B}-\mathrm{A})}{(\mathrm{C}+\mathrm{B}+\mathrm{A})} \qquad \mathrm{HR2} = \frac{(\mathrm{C}-\mathrm{B})}{(\mathrm{C}+\mathrm{B})}.$$

We select all detections with $\mathrm{HR1} \leq -0.5$ from both catalogs. After this selection only $\sim$5% of the original catalog remains of interest. This list is further condensed by looking for multiple detections of the same object. In the end, 4101 individual SXS remain to be identified; we define this as the "parent sample".

A literature search was conducted for each object in the parent sample, both through the SIMBAD database and catalogs compiled at MIT. In the end, about 500 sources could be identified through such literature searches[1], leaving over 3500 sources to be identified with optical counterparts. It is not feasible to carry

[1] The literature search is an on-going process. We are continually seeking and searching additional catalogs.

out so many observations in a reasonable amount of time. To effectively achieve our goals, we have defined four (occasionally overlapping) subsamples.

Our goal is to observe 90% of the sources in each subsample and determine whether or not they are NBWD. The exception is the flux limited sample where we demand an optical counterpart to the SXS independent of the system type.

2.1 Flux Limited Sample

In order to determine what proportion of the SXS are of various classes (CVs, AGN, etc.) in a statistically meaningful way, we have defined a flux limited sample of SXS. In this sample we restrict ourselves to the WGA catalog because of the careful consideration of point spread function effects for sources far off-axis (Haberl et al. 1994). Care has been taken to select objects with similar exposure times and interstellar absorption characteristics such that the ROSAT PSPC count rate can be used as a measure of flux. The resultant log(dN/dS)-log(S) plot is shown in Fig. 1. We have chosen a (conservative) lower flux limit of 0.014 cnts/s; Fig. 1 indicates that the X-ray data are complete to even lower flux values. This sample covers ≈120 square degrees of sky and contains 177 sources.

In addition to determining the constituency of the SXS, the flux limited sample will serve as a basis for studying SXS AGN. Table 2 (presented in Section 4) indicates that we will identify a large number SXS AGN from which we will be able to determine a luminosity function. We will look for signs of evolution in this distribution and compare it to other luminosity functions of general X-ray selected AGN.

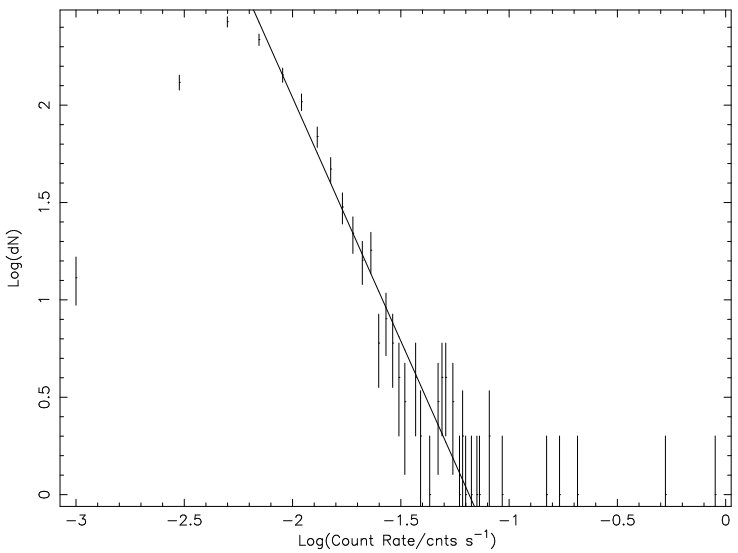

Fig. 1. Log(dN/dS)-Log(S) plot for the flux limited sample. A -5/2 power law is shown. We take a conservative completeness limit of 0.014 counts/s.

2.2 Extremely Soft Sample

To be classified as "supersoft" in this work, a source requires an HR1 value of ≤ -0.5 (75% of the counts in band A); however, there are a number of reasons to consider the very softest sources with HR1 ≤ -0.8 (90% of the counts in band A) distributed over the entire sky. To begin, NBWD systems are very soft, and it is a stated goal of this program to find more of these systems. In fact many of the known NBWD systems have been found in this range. Next the 0.1 – 0.4 keV region is being explored with great sensitivity for the first time with the ROSAT satellite. Therefore the identification of sources in this band is potentially rich in new phenomena. This sample includes 355 SXS.

2.3 Optically Bright Sample

Due to the very soft X-ray spectrum of a NBWD, any such object in the Milky Way detected by ROSAT is probably quite local because interstellar attenuation of soft X-rays would make more distant sources undetectable. At the same time, NBWD can be very luminous ($\sim 10^{38}$ erg/s). The combination of these properties might well result in an optically bright counterpart. For example RX J0019.8+2156, the only unobscured galactic NBWD known, has $m_V \sim 12.8$ (Beuermann et al. 1995). The opportunities that would arise from the discovery and study of a new NBWD system have prompted us to define a sample of all stars brighter than $V \sim 14.5$ within 1.3 error radii of the X-ray position (at 1.3 error radii the optical counterpart should be enclosed with a probability of 96%). A comparison of the parent sample to the Space Telescope Guide Star Catalog (ST-GSC) yields 694 stars meeting these criteria, distributed among 640 SXS. Although the ST-GSC is generally complete to 14.5 magnitude, this limit can can be significantly worse for dense fields. In these cases we attempt to include stars neglected in the ST-GSC via direct inspection of the finding charts produced with the Digital Sky Survey.

2.4 NBWD Track Sample

We also take another approach to finding galactic NBWDs among the 80,000 detections in the WGA and SRC catalogs, by generating a simulated catalog with only a population of NBWD distributed throughout the Milky Way. Using a simple "disk + bulge" model for interstellar gas, the column density to any point in the simulated galaxy can be analytically determined. The NBWD are placed in a disk population with a space density that decays exponentially with height above the midplane. The scale heights for the NBWDs and gas are taken to have the ratio $z_{\rm NBWD}/z_{\rm gas} = 0.5$ (following Di Stefano & Rappaport 1994), and their spectra (taken to be simple blackbodies) are selected from a luminosity-temperature distribution determined by (Rappaport & Di Stefano 1994). The probability of choosing any given (L,T) was weighted by the expected lifetime of that system.

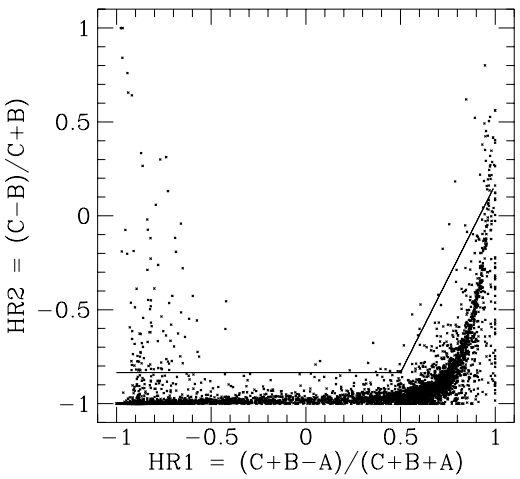

Fig. 2. Distribution of simulated galactic NBWD in the HR1-HR2 plane. 5000 "detections" from 46,464 seeded systems are plotted.

The intrinsic spectrum from each NBWD is modified by interstellar absorption, then "observed" by folding the incident spectrum through the ROSAT PSPC response matrix.

In order to be consistent with the actual catalogs, after including the effects of background and Poisson noise, we demand a signal-to-noise ratio $\geq$5.0 to be secure in a detection. Only the count rate and the number of counts in channels A, B and C are accumulated. The goal is to find relations among these spectral parameters which constrain the parameter space that is likely to contain Galactic NBWD.

Fig. 2 shows a very clear relation between HR1 and HR2 which agrees very well with known nuclear burning white dwarf systems. Based on this result, we are currently defining a fourth sample (the area below the line in Fig. 2) to optimize our search for NBWD[2].

3 Current Status

At the time this article was written we were about half way through the observing program. In about 50 nights of observing time we have taken 939 spectra, all but 5 on the Michigan - Dartmouth - MIT (MDM) 1.3 meter observatory atop Kitt Peak, Arizona. An additional 20 nights are scheduled in the first half of 1996.

Table 1 shows our progress on each subsample. The optically bright sample is virtually complete. The flux limited sample needs the most work; however, this sample was least conducive to study with the MDM 1.3m. Upcoming time on the MDM 2.4m should be highly productive in this regard. Note we are taking a very strict approach to "new identification" at this time, requiring compelling evidence that the counterpart has been found (e.g. emission lines, optical flux, and/or spatial coincidence with the X-ray position) Most notably we have not

[2] Other researchers have independently drawn similar conclusions utilizing other methods (e.g., Motch et al. 1994 and Kahabka 1996).

Table 1. Current status of the sub-samples

Sample	Total Sources	To Be Observed	Total IDs	New IDs	Literature IDs
Flux Limited	177	148	30	10	20
Extremely Soft	355	203	150	5	145
Optically Bright	694	134	147	13	134
Other	3035	2746	289	18	271

finished analyzing the ordinary stars, over 200 of which are probably optical identifications. This uncertainty is also reflected in Table 2 below.

4 Preliminary Results

A brief summary of our results to date is shown below in Tab. 2; general trends can be extracted from this information. The trends found in the RASS sample of SXS toward large numbers of SXS AGN (Greiner et al. 1996) and a predominance of SXS CVs being of the AM Her type (Beuermann & Burwitz 1995) continue to hold in the pointed survey.

Each sub-sample tends to have its own "signature class". The flux limited sample is dominated by SXS AGN (20 of 30 identified systems), The extremely soft sample is predominately white dwarfs and AM Her CVs, and the optically bright sample consists mainly of active coronae stars with notable numbers of white dwarfs. Note many of the sources in the optically bright sample have not tabulated at the moment and many of these are exepected to be active coronae stars.

New identifications are being made at a steady pace, mainly among AGN and emission stars. The fact that we have not made more firm identifications stems from a few things. Most of our observations have taken place on the MDM 1.3m during bright time. Next, the CCD used in most of the observations does not have sufficient blue response to examine the CaII H and K lines ($\lambda\lambda 3933, 3969$) which are excellent indicators of active coronae. As a result we have focused on the optically bright sample (see Table 1) which could be most easily carried out under these conditions. The Spring 1996 runs have been optimized to explore the other samples where actual identifications are the goal.

An example of the type of spectra we are accumulating during this project is shown for SXS AGN in Fig. 4. The spectra of four newly identified sources (at a variety of redshifts) are plotted in the figure. In addition to the obvious emission lines, iron emission complexes are noted on either side of the [OIII] doublet. These features are found in most of our SXS AGN and may signify the presence of dense, cool regions in the system, perhaps forming in parallel with the warm absorber. However, note there is nothing obviously different on the optical spectra of SXS AGN compared to the diverse varieties (e.g. emission

Table 2. Current SXS identifications by class and subsample

Class	Total (New)	Flux	Soft	Optical	Other
AGN (QSO)	78 (9)	12	5	1	60
AGN (Seyferts)	31 (14)	6	0	4	21
AGN (Other)	8 (0)	2	0	0	6
White Dwarfs	94 (5)	2	86	35	3
Emission Stars	44 (22)	3	12	20	15
CV (AM-Her)	19 (0)	3	16	0	3
CV (DQ-Her)	2 (0)	1	1	1	0
CV (Nova Like)	1 (0)	1	0	1	0
CV (Unclassified)	1 (1)	0	0	0	1
CSPN	5 (0)	0	3	2	2
Symbiotic Stars	3 (0)	0	3	2	0
Pulsars	3 (0)	0	1	0	2
Novae	2 (0)	0	1	1	1
Nuclear Burning WD	2 (0)	0	1	1	1
Early Stars (O1-F5)	>36 (?)	0	6	22	5
Late Stars (F6-M9)	>89 (?)	0	15	57	23

line ratios) in hard X-ray selected samples. The combination of optical and X-ray spectra will help us determine the physical mechanisms responsible for the 0.1–0.4 keV emission. A supporting SAX proposal has been submitted.

Finally, we note that we have yet to find a new NBWD; however, we will be looking in the southern hemisphere for the first time during spring, 1996. This, in combination with the new "NBWD Track selected sample" improves our chances of finding new systems of this type.

5 Summary

The WGA and SRC catalogs provide a complementary data set to the RASS, trading sky coverage for a factor of ∼20 in average exposure time. We are halfway through a two-year program to identify SXS in the pointed catalogs. At this point, we can confirm that the RASS results regarding AM Her CVs (this subclass dominates all SXS CVs) and AGN (there are more SXS AGN than previously thought) still hold in our work. Although no new NBWDs have been found, we have made steady progress identifying new optical counterparts to SXS, most of which are AGN and emission stars.

Acknowledgements: This work is supported by funds of NASA ADP grant NAG5-3011 and NASA ROSAT guest observer grant NAG5-1784. In addition special thanks to the MDM observatories for time and technical support, the MPE ROSAT group for the SRC catalog, the White group at GSFC for the WGA catalog, and the CDS at Strausbourg, France for access to the SIMBAD database.

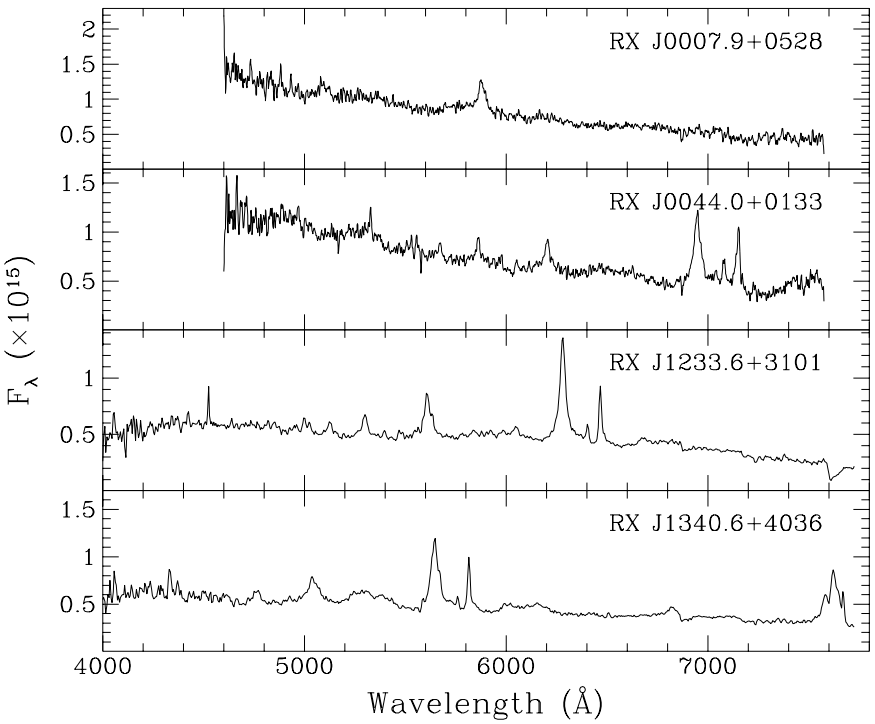

Fig. 3. Optical spectra of four newly identified SXS AGN. The redshifts (top to bottom) are 1.1, 0.44, 0.29, and 0.16.

References

Beuermann K., Reinsch K., Barwig H., et al. 1995, A&A 294, L1

Beuermann K., Burwitz V., 1995, in Cape Workshop on Magnetic Cataclysmic Variables, ASP Conf. Proceedings 85, eds. D.A.H Buckley & B. Warner

DiStefano R., Rappaport S., 1994, ApJ 437, 733

Greiner J., Danner R., Bade N. et al. 1996, A&A, (in press)

Haberl F., Pietsch W., Voges W., 1994, "Differences in the Two ROSAT Catalogs of Pointed PSPC Observations" WWW Document, *http://rosat_svc.mpe-garching.mpg.de/rosat_svc/archive/sourcecat/wga_rosatsrc.html* (26 March 1996)

Kahabka P., 1996, this volume p. 215

Motch C., Hasinger G., Pietsch W., 1994, A&A 284, 827

Rappaport S., DiStefano R., Smith J.D., 1994, ApJ 426, 692

White N., Giommi P., Angellini L., 1994, IAUC 6100

Zimmerman H.-U., 1994, IAUC 6102